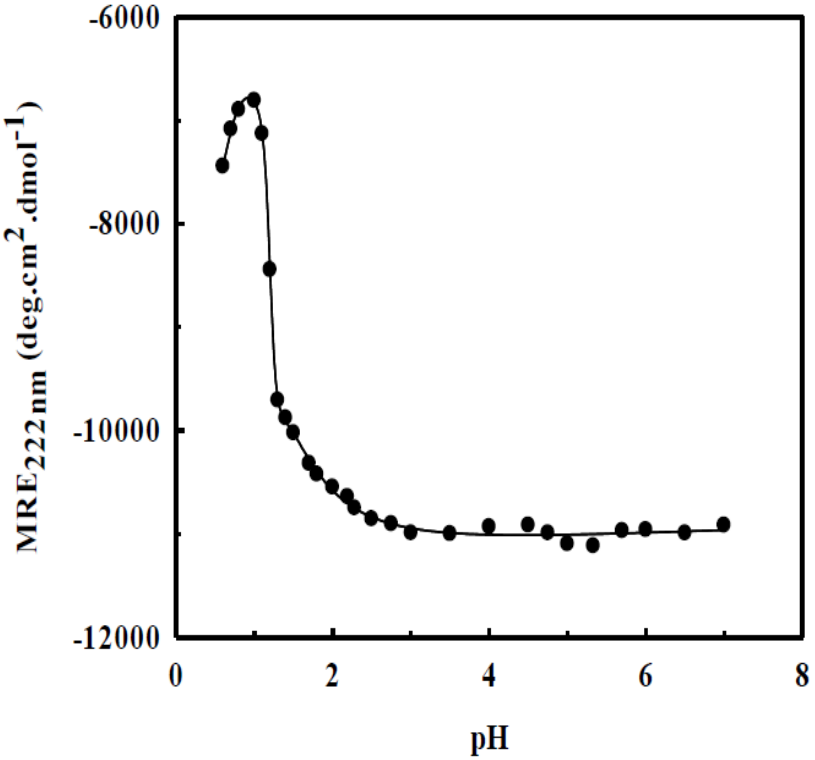

Figure 4.1. Change in the far-UV CD spectral signal, MRE_{222nm} of glucoamylase as a function of pH at 25ºC. The protein concentration used was 1.4 μM. Experimental conditions were the same as described in the Materials and Methods.

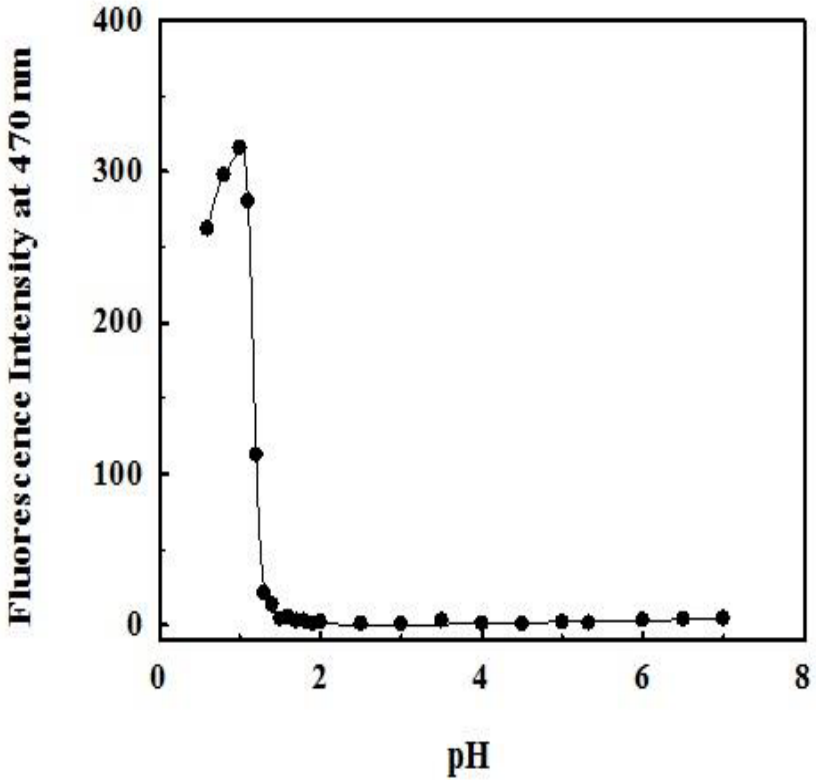

Figure 4.2. Change in the ANS fluorescence intensity at 470 nm of glucoamylase as a function of pH at 25ºC. The protein concentration used was 0.26 μM, whereas the ANS concentration was 18 μM. Experimental conditions were the same as described in the Materials and Methods.

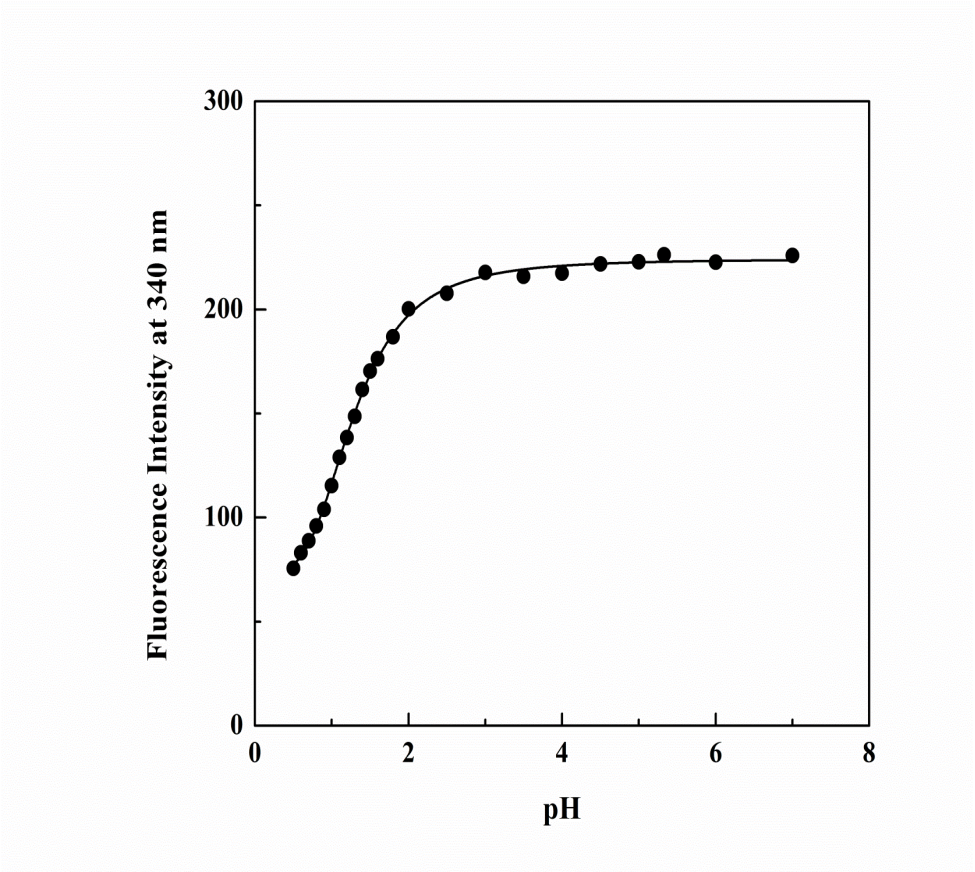

Figure 4.3. Plot showing change in the Trp fluorescence intensity at 340 nm of glucoamylase as a function of pH at 25ºC. The protein concentration used was 0.12 μM and the protein solution was excited at 295 nm. Experimental conditions were the same as described in the Materials and Methods.

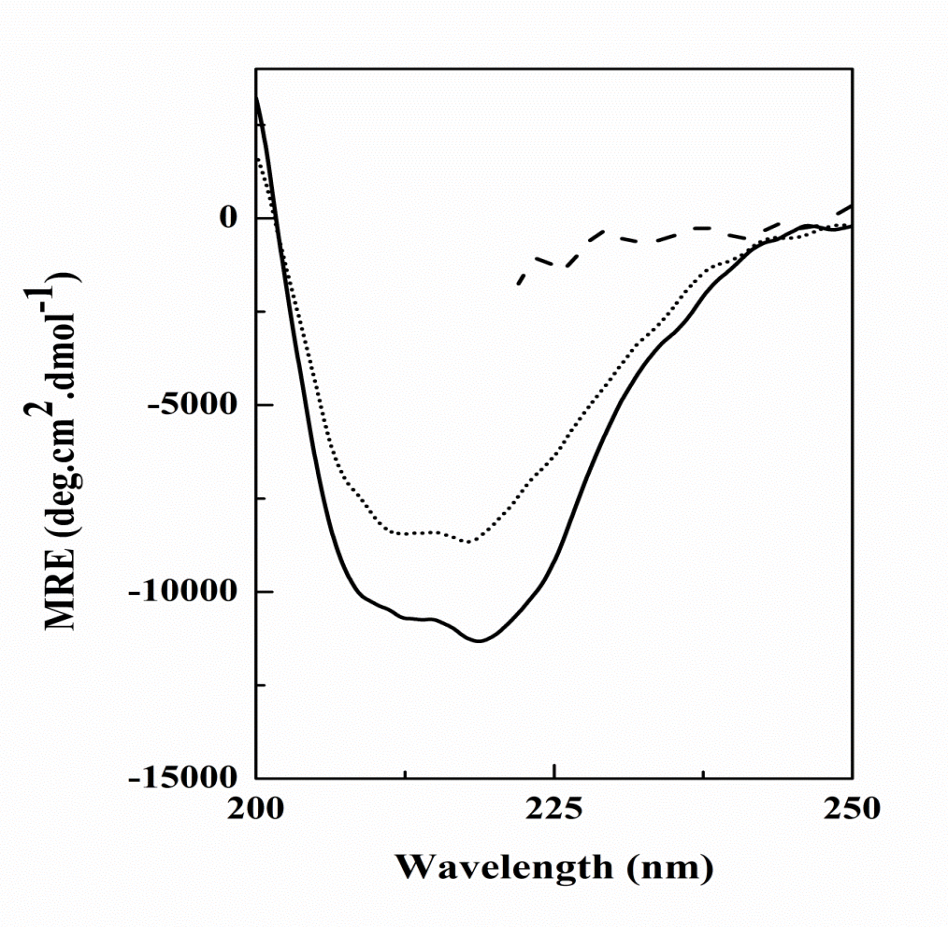

Figure 4.4. Far-UV CD spectra of different states of glucoamylase obtained at 25ºC,using a protein concentration of 1.4 μM. Native state at pH 7.0 (——), acid-denatured state at pH 1.0 (·····) and 6.0 M GdnHCl-denatured state (– – –).

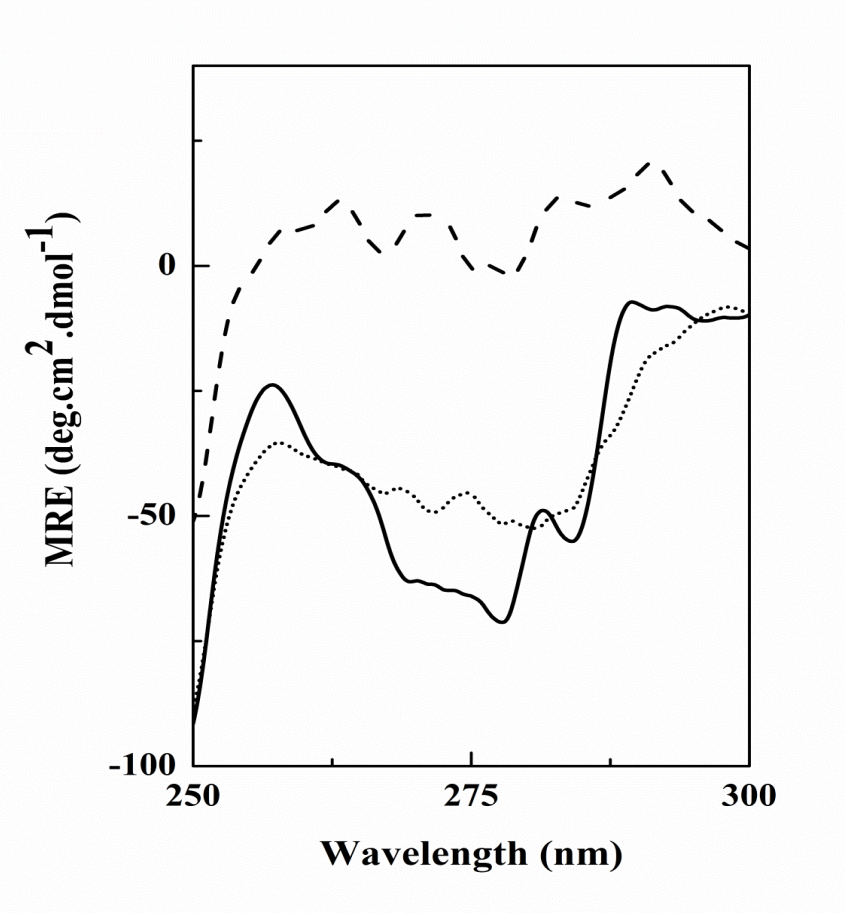

Figure 4.5. Near-UV CD spectra of different states of glucoamylase obtained at 25ºC, using a protein concentration of 12 µM. Native state at pH 7.0 (——), acid-denatured state at pH 1.0 (·····) and 6.0 M GdnHCl-denatured state (– – –).

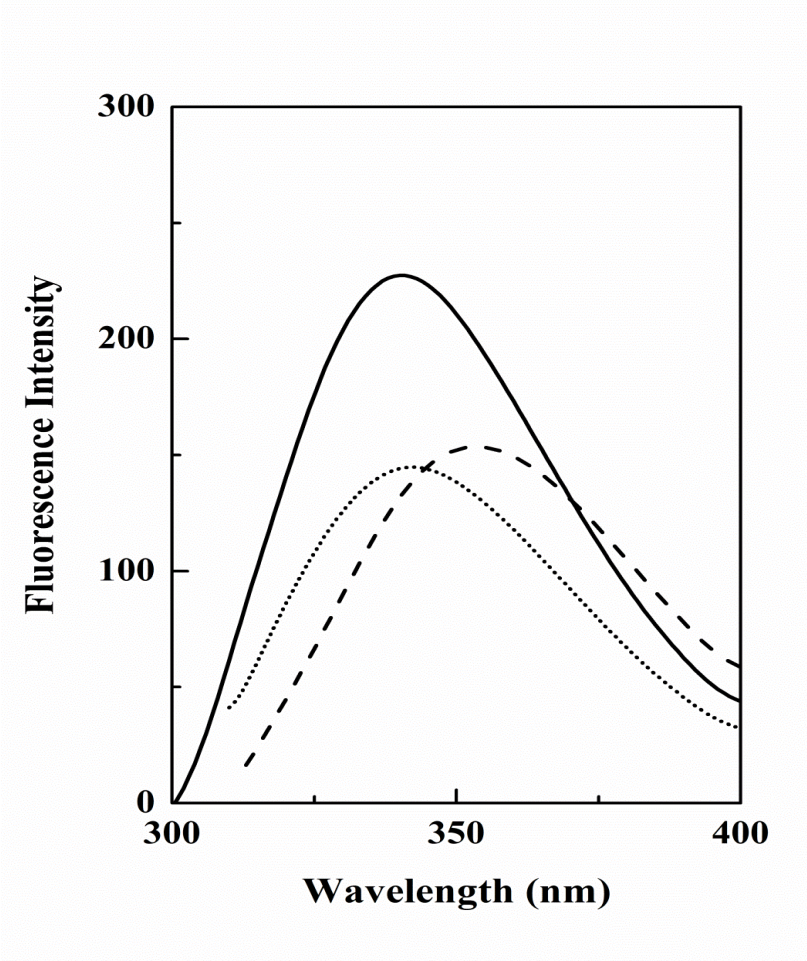

Figure 4.6. Trp fluorescence spectra of different states of glucoamylase obtained at 25ºC, using a protein concentration of 0.12 μM. The excitation wavelength used was 295 nm. Native state at pH 7.0 (——), acid-denatured state at pH 1.0 (·····) and 6.0 M GdnHCl-denatured state (– – –).

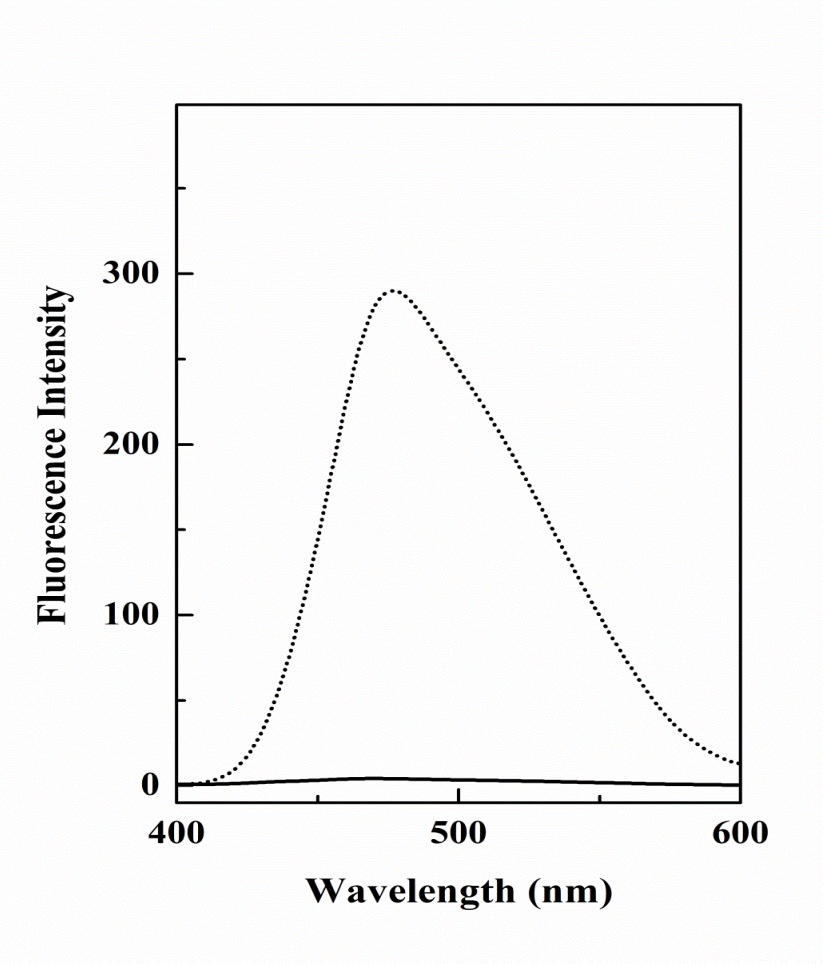

Figure 4.7. ANS fluorescence spectra of different states of glucoamylase obtained at 25ºC, using a protein concentration of 0.26 μM. The excitation wavelength used was 380 nm, whereas the ANS concentration was 18 μM. Native state at pH 7.0 (——) and the acid-denatured state at pH 1.0 (·····).

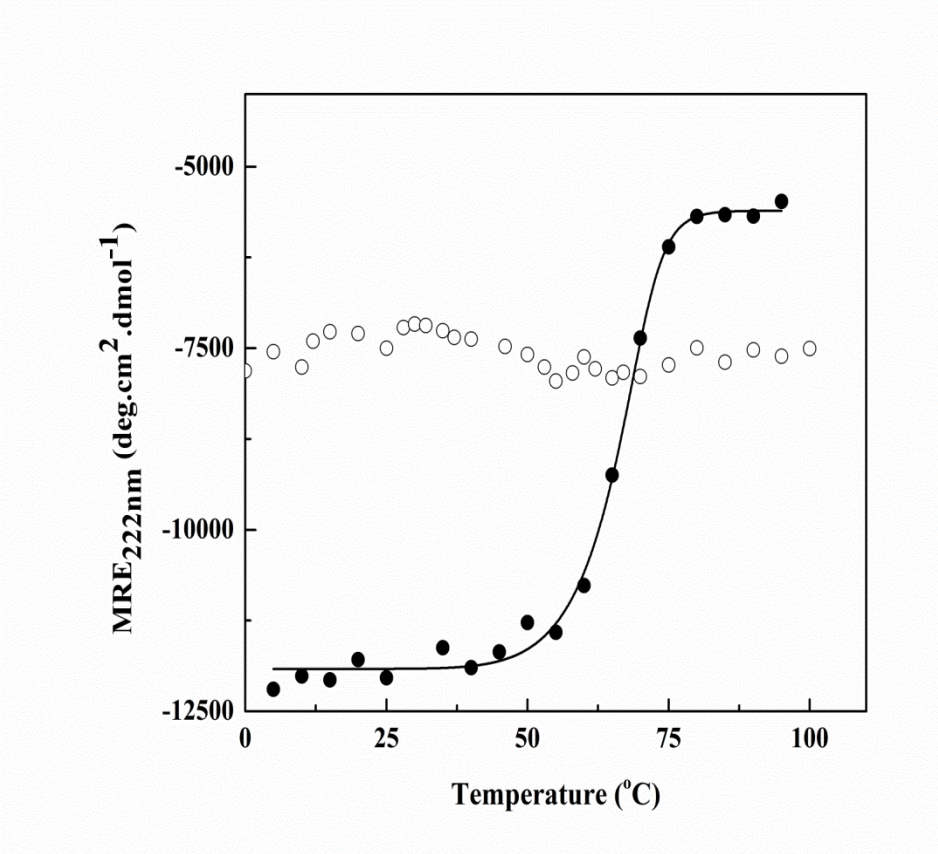

Figure 4.8. Temperature-dependence of far-UV CD spectral signal, MRE_{222nm} of the native state at pH 7.0 (●) and the acid-denatured state at pH 1.0 (○) of glucoamylase. The protein concentration used was 1.4 μM.

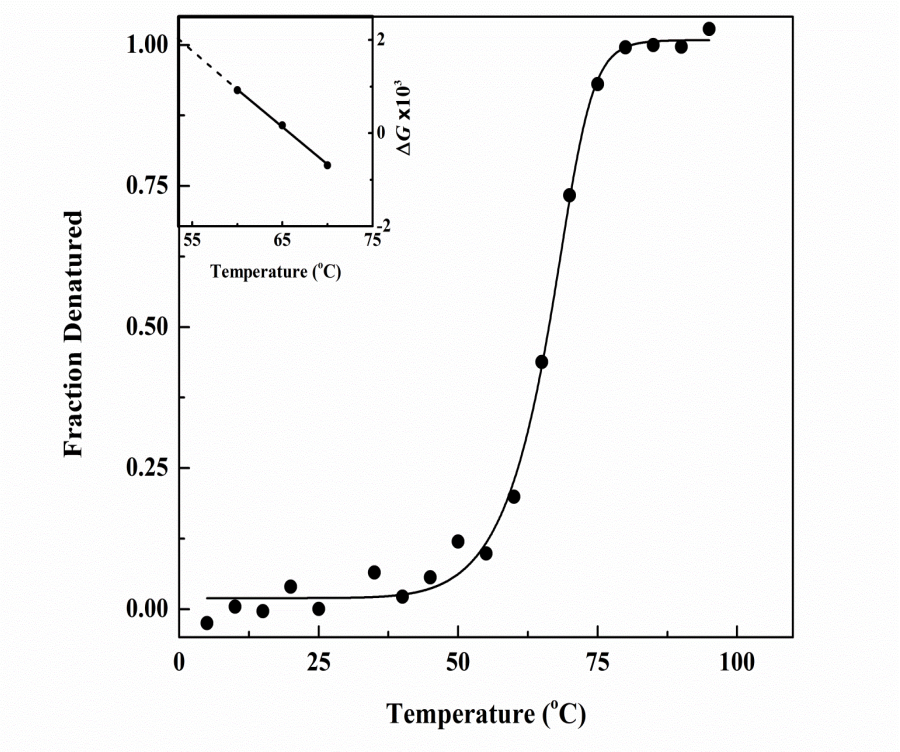

Figure 4.9. Normalized transition curve for thermal denaturation of glucoamylase at pH 7.0 as shown in Figure 4.8. Inset shows the plot of ΔG versus temperature.

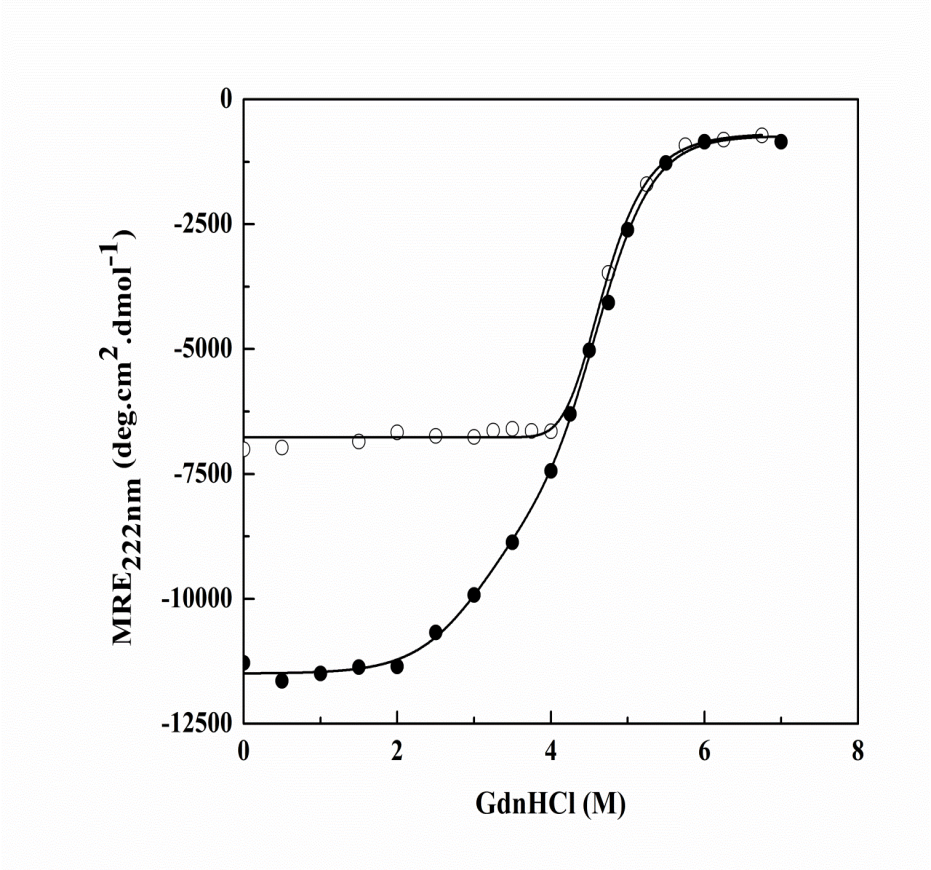

Figure 4.10. GdnHCl-induced denaturation of glucoamylase at pH 7.0 (●) and pH 1.0 (○), as monitored by far-UV CD spectral signal, MRE_{222nm} using a protein concentration of 1.4 μM.

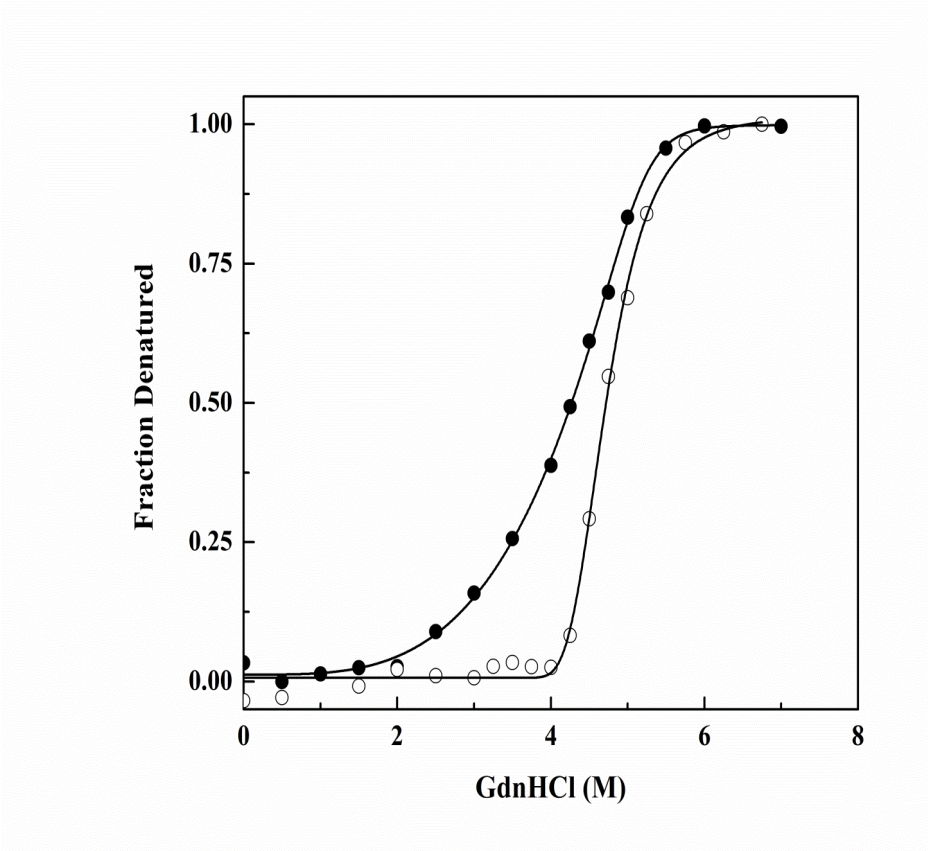

Figure 4.11. Normalized curves for GdnHCl denaturation of the native (●) and the acid-denatured (○) glucoamylases for the transitions shown in Figure 4.10.

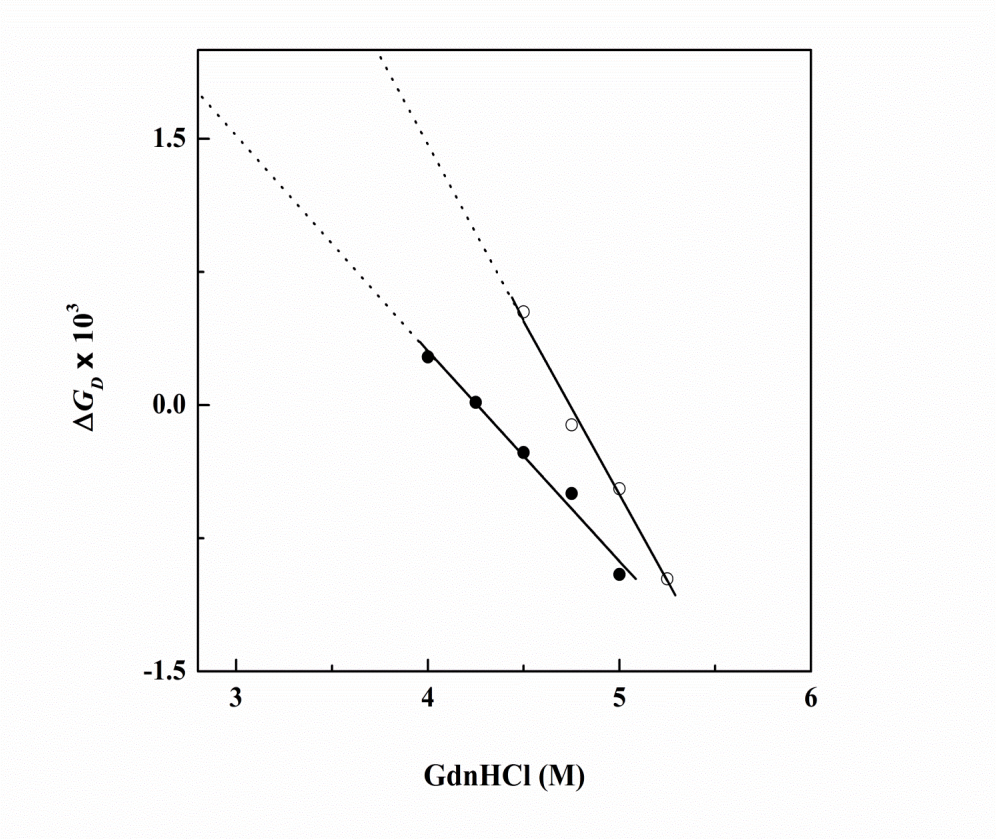

Figure 4.12. Linear plots showing dependence of ΔG_D on GdnHCl concentration for the native (●) and the acid-denatured (○) glucoamylases.

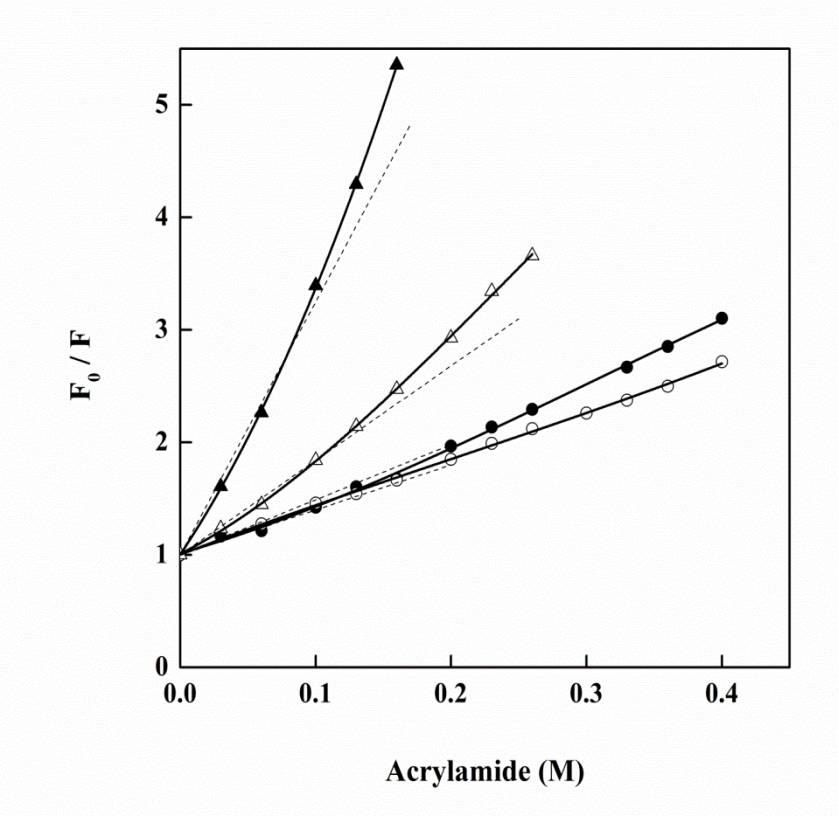

Figure 4.13. Stern-Volmer plots of acrylamide quenching of the native state at pH 7.0 (○), the acid-denatured state at pH 1.0 (●) and the 6.0 M GdnHCl-denatured state (Δ) of glucoamylase as well as NATA (▲) as studied at 25ºC. F_0 and F represent fluorescence intensities observed in the absence and presence, respectively, of acrylamide. Dotted lines represent theoretical curves by fitting to Eq. (4).

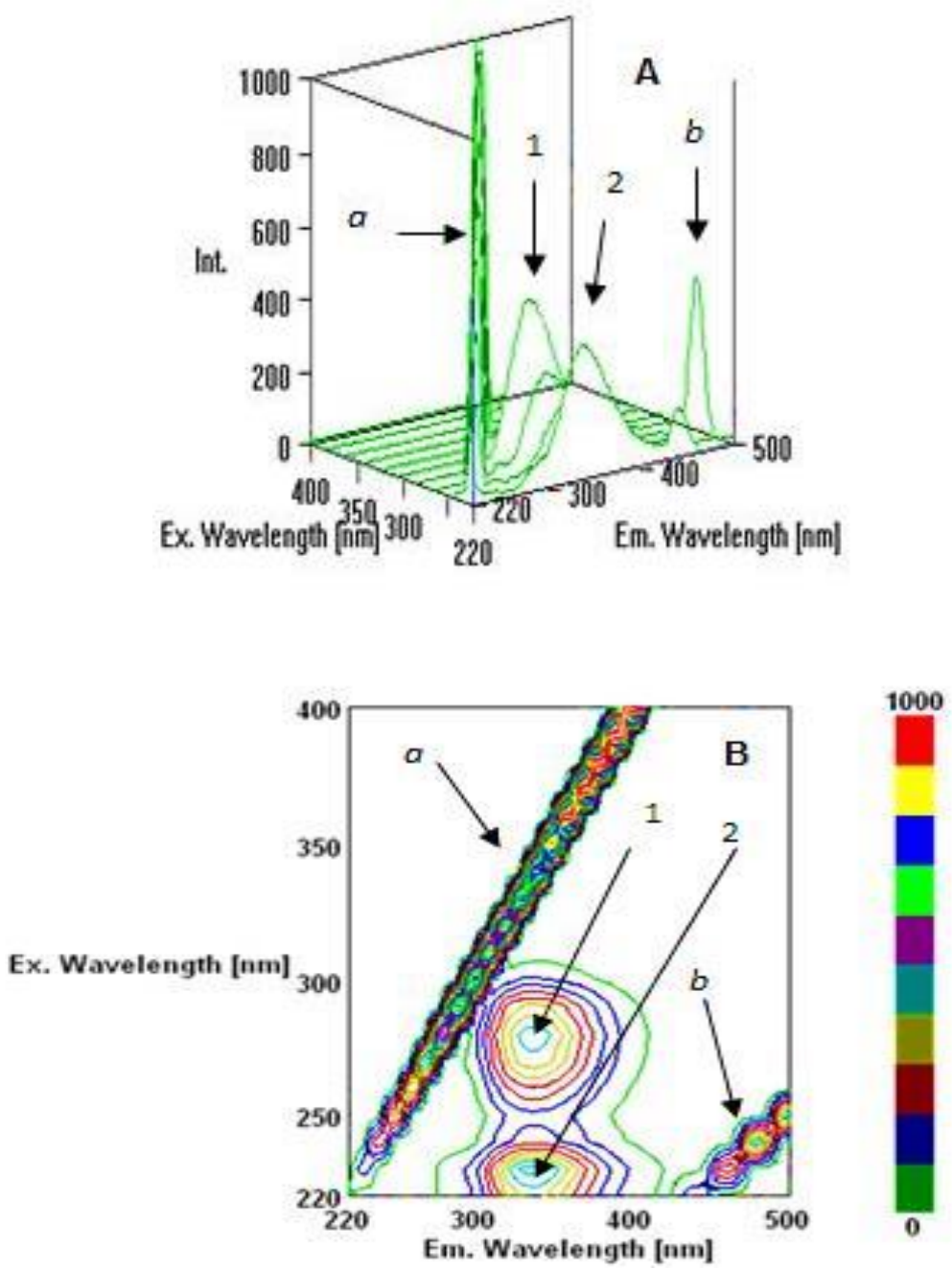

Figure 4.14. Three-dimensional fluorescence spectra (A) and corresponding contour map (B) of the native state of glucoamylase, using a protein concentration of 0.12 μM.

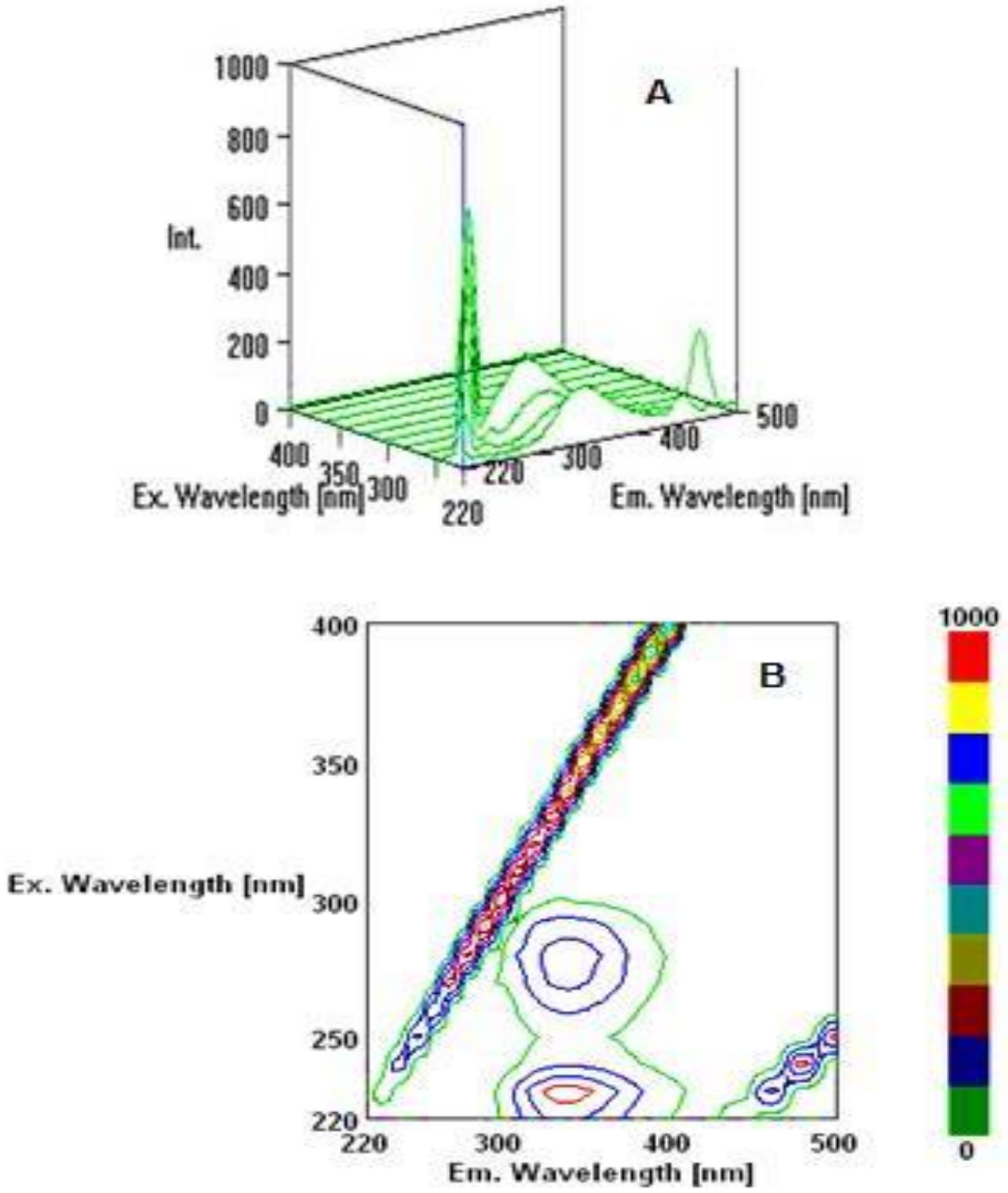

Figure 4.15. Three-dimensional fluorescence spectra (A) and corresponding contour map (B) of the acid-denatured state of glucoamylase, using a protein concentration of 0.12 μM.

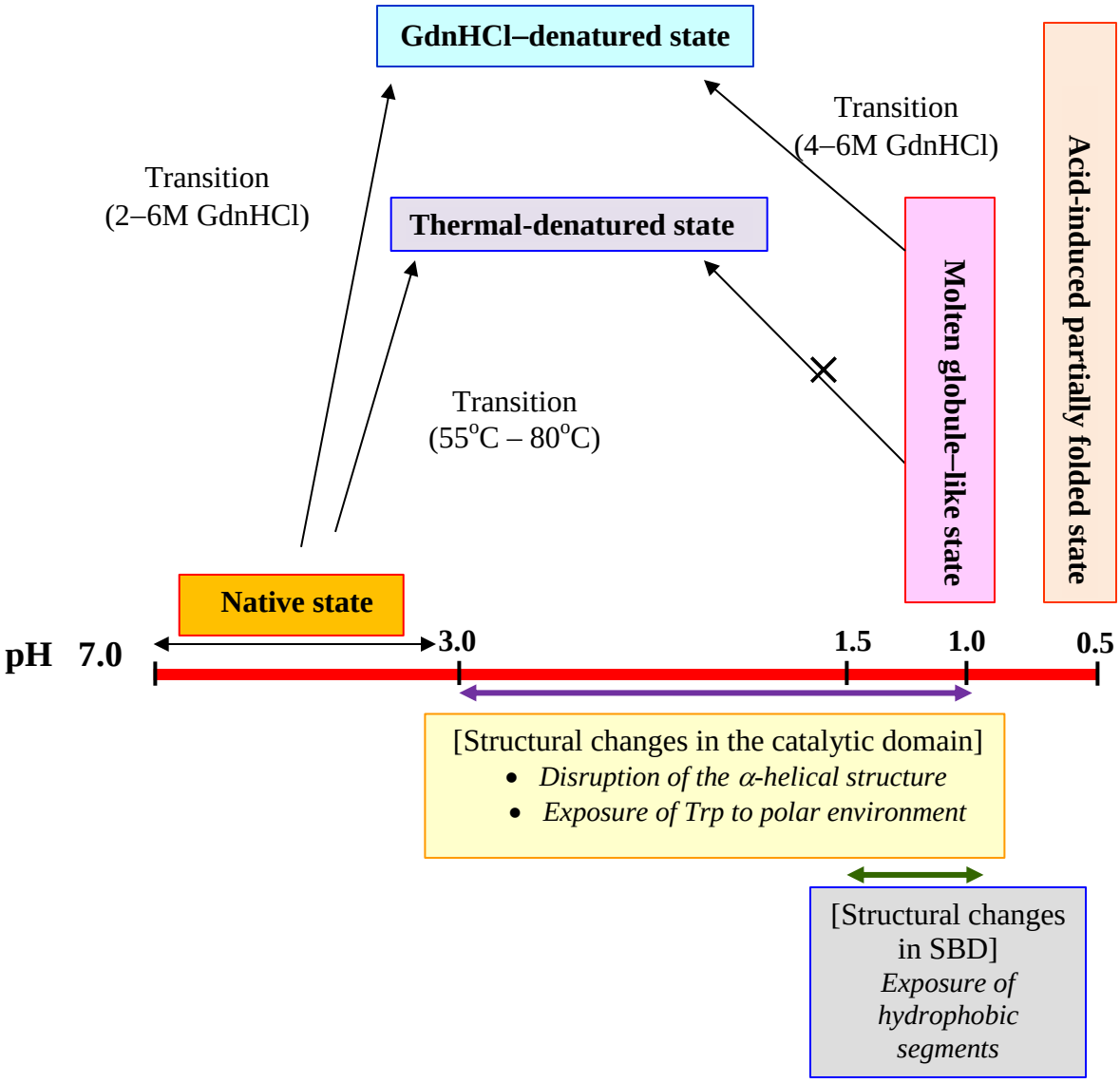

Figure 4.16. Scheme showing proposed unfolding pathway of glucoamylase as monitored by acid-induced conformational changes and comparison of the molten globule-like state with the native state with respect to thermal and GdnHCl denaturations.

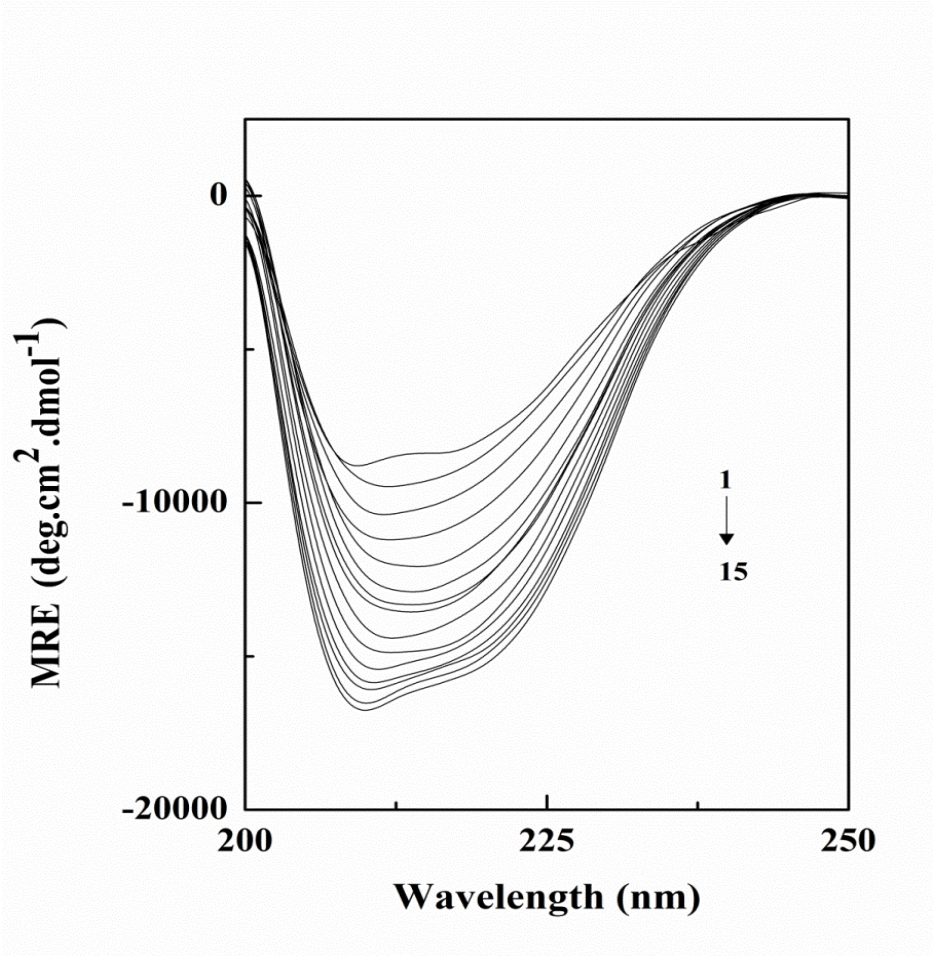

Figure 4.17. Far-UV CD spectra of the acid-denatured glucoamylase obtained in 10 mM glycine-HCl buffer, pH 1.0 both in the absence and presence of increasing concentrations of TFE. The TFE concentrations (from top to bottom) were: 0, 0.5, 1.0, 1.5, 2.0, 3.0, 4.0, 4.5, 5.0, 5.5, 6.0, 6.5, 7.0, 7.5 and 8.0 M, respectively. The CD measurements were performed at 25ºC, using a protein concentration of 1.4 μM.

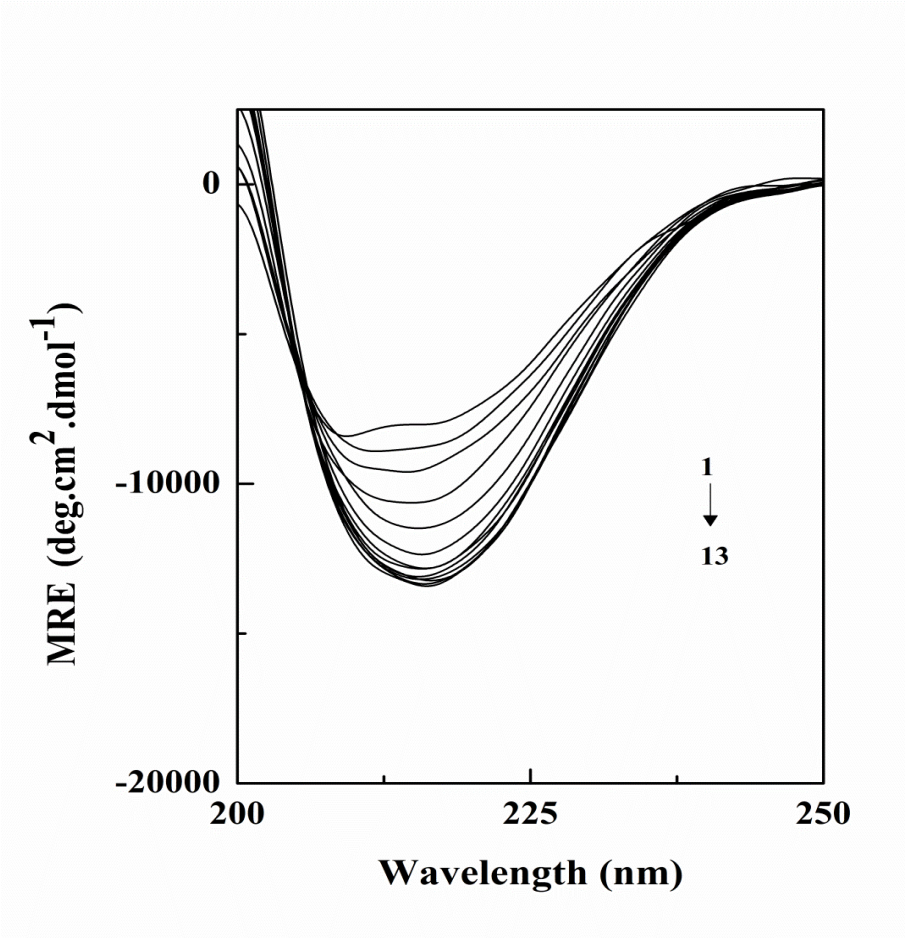

Figure 4.18. Far-UV CD spectra of the acid-denatured glucoamylase obtained in 10 mM glycine-HCl buffer, pH 1.0 both in the absence and presence of increasing concentrations of tert-butanol. The tert-butanol concentrations (from top to bottom) were: 0, 0.5, 1.0, 1.5, 2.0, 2.5, 3.0, 3.5, 4.0, 4.5, 5.0, 5.5, and 6.0 M, respectively. The CD measurements were performed at 25ºC, using a protein concentration of 1.4 μM.

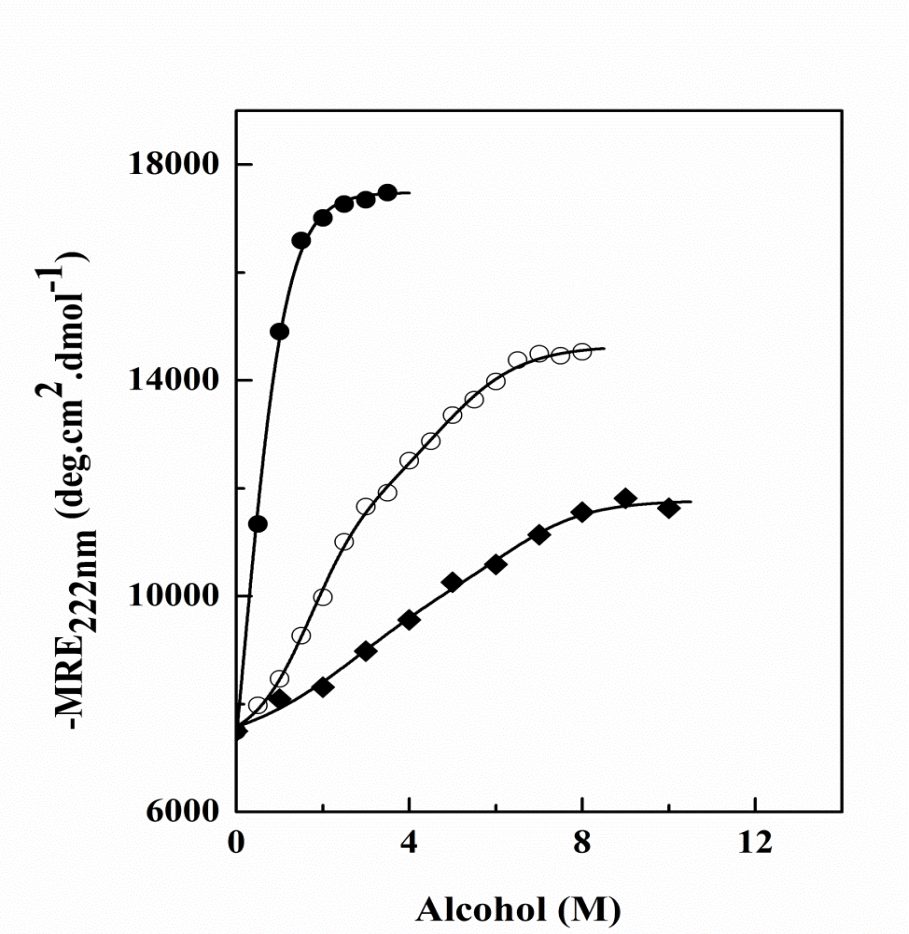

Figure 4.19. Halogenol-induced structural transitions of the acid-denatured glucoamylase at pH 1.0 (25ºC) as monitored by MRE_{222nm} measurements, using a protein concentration of 1.4 μM. Various symbols shown in the figure refer to: HFIP (●), TFE (○) and 2-chloroethanol (♦).

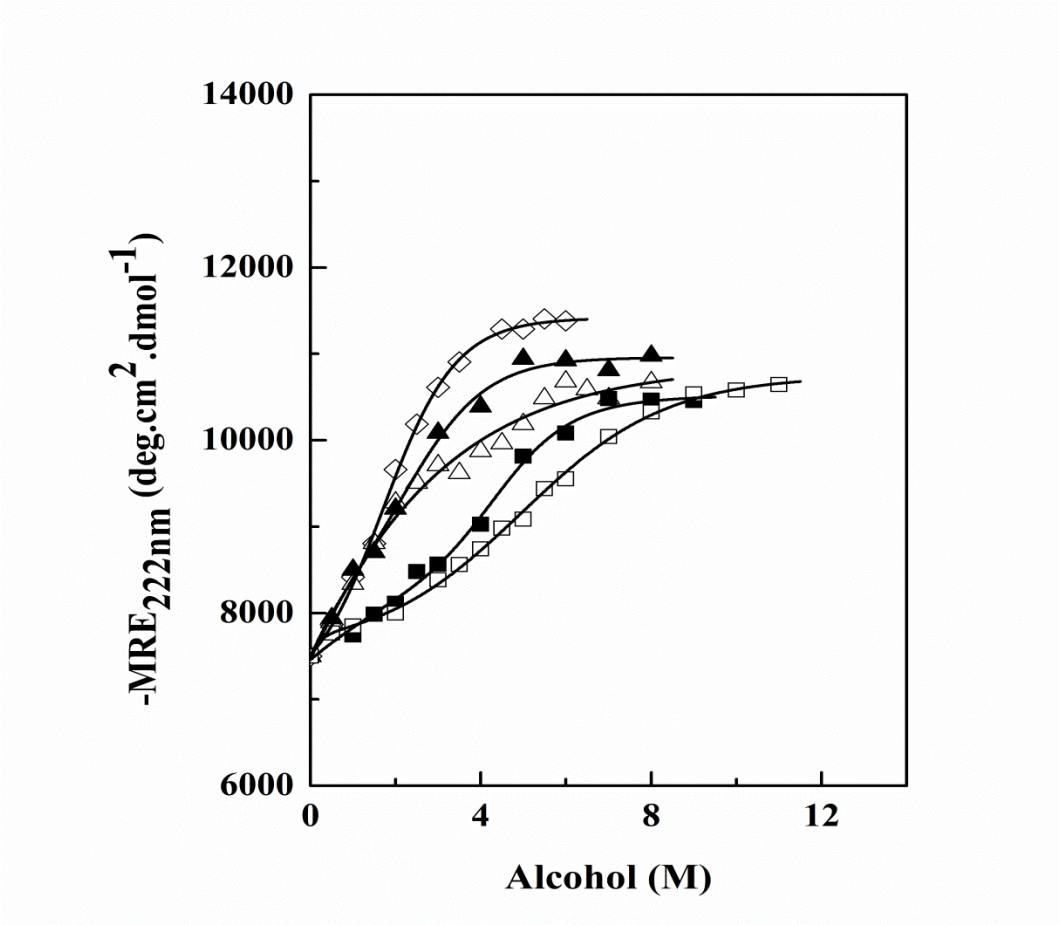

Figure 4.20. Alkanol-induced structural transitions of the acid-denatured glucoamylase at pH 1.0 (25ºC) as monitored by MRE_{222nm} measurements, using a protein concentration of 1.4 μM. Various symbols shown in the figure refer to: tert-butanol (◊), 1-propanol (▲), 2-propanol (Δ), ethanol (■) and methanol (□).

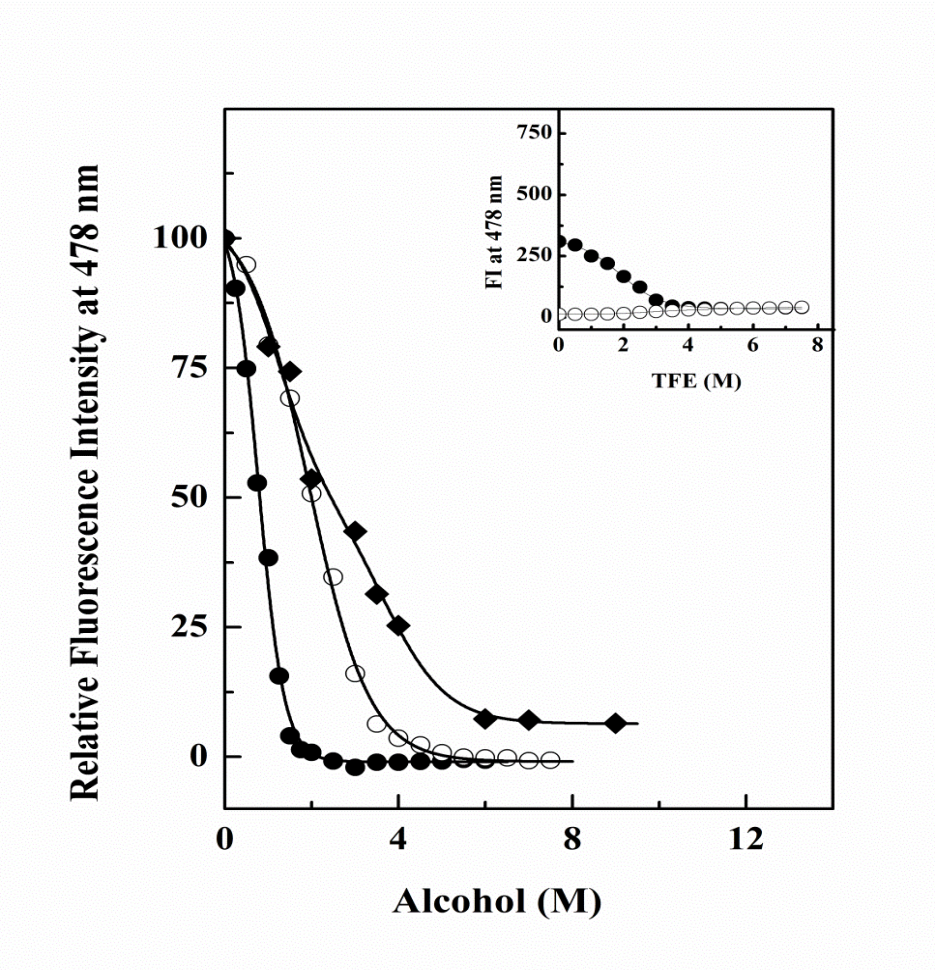

Figure 4.21. Halogenol-induced structural transitions of the acid-denatured glucoamylase at pH 1.0 (25ºC) as monitored by ANS fluorescence measurements at 478 nm, using a protein concentration of 0.26 μM. Various symbols shown in the figure refer to: HFIP (●), TFE (○) and 2-chloroethanol (♦). Inset shows variation in the ANS fluorescence intensity (FI) at 478 nm both in the absence (○) and presence (●) of glucoamylase with increasing concentrations of TFE.

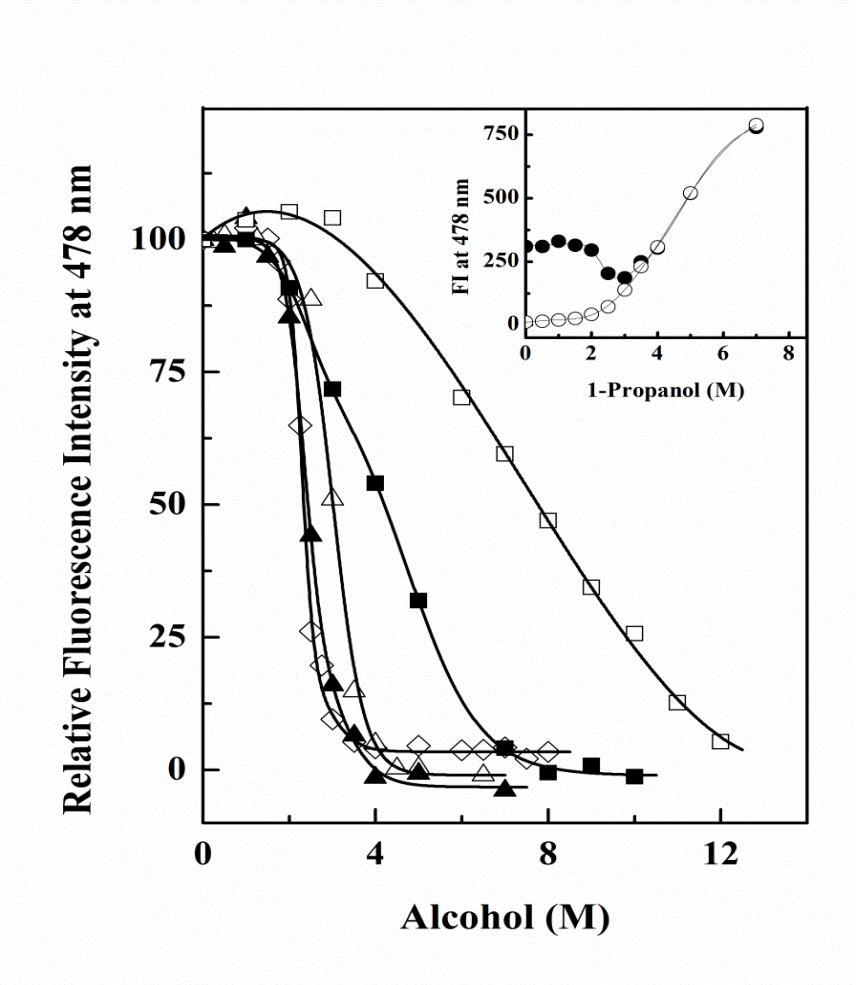

Figure 4.22. Alkanol-induced structural transitions of the acid-denatured glucoamylase at pH 1.0 (25ºC) as monitored by ANS fluorescence measurements at 478 nm, using a protein concentration of 0.26 μM. Various symbols shown in the figure refer to: tert-butanol (◊), 1-propanol (▲), 2-propanol (Δ), ethanol (■) and methanol (□). Inset shows variation in the ANS fluorescence intensity (FI) at 478 nm both in the absence (○) and presence (●) of glucoamylase with increasing concentrations of 1-propanol.

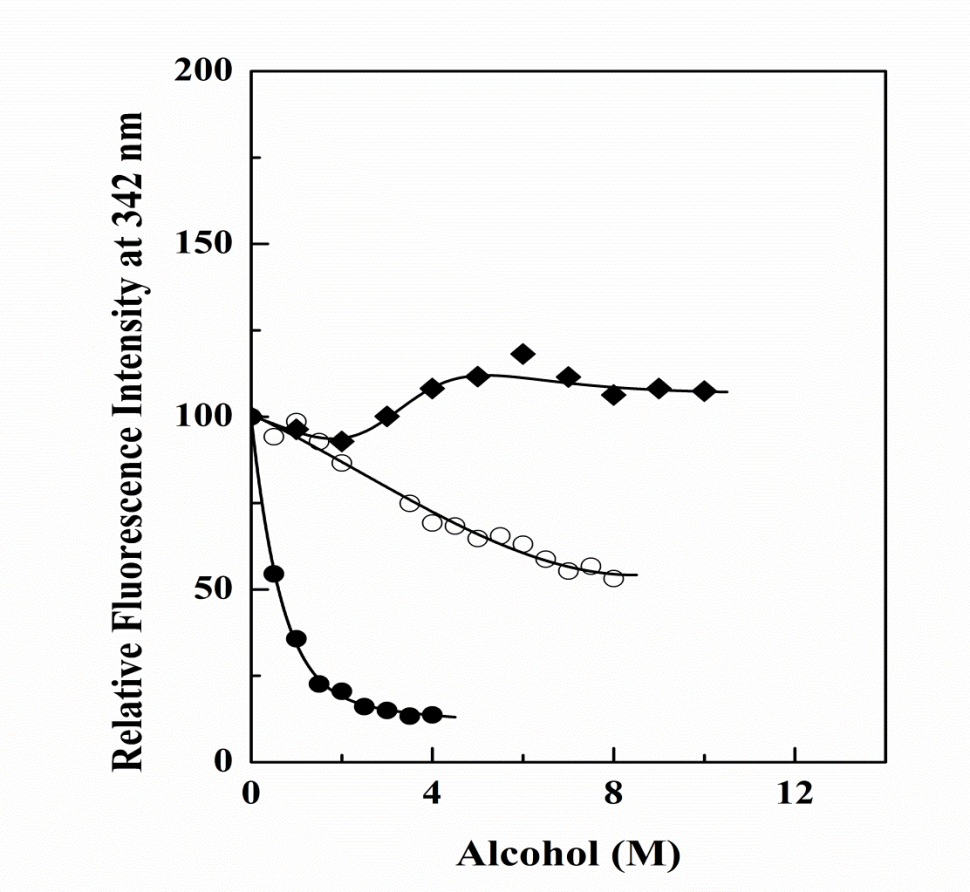

Figure 4.23. Conformational transitions of the acid-denatured glucoamylase at pH 1.0 (25ºC) induced by halogenols as monitored by Trp fluorescence measurements at 342 nm (excitation wavelength = 295 nm), using a protein concentration of 0.12 μM. Various symbols shown in the figure refer to: HFIP (●), TFE (○) and 2-chloroethanol (♦).

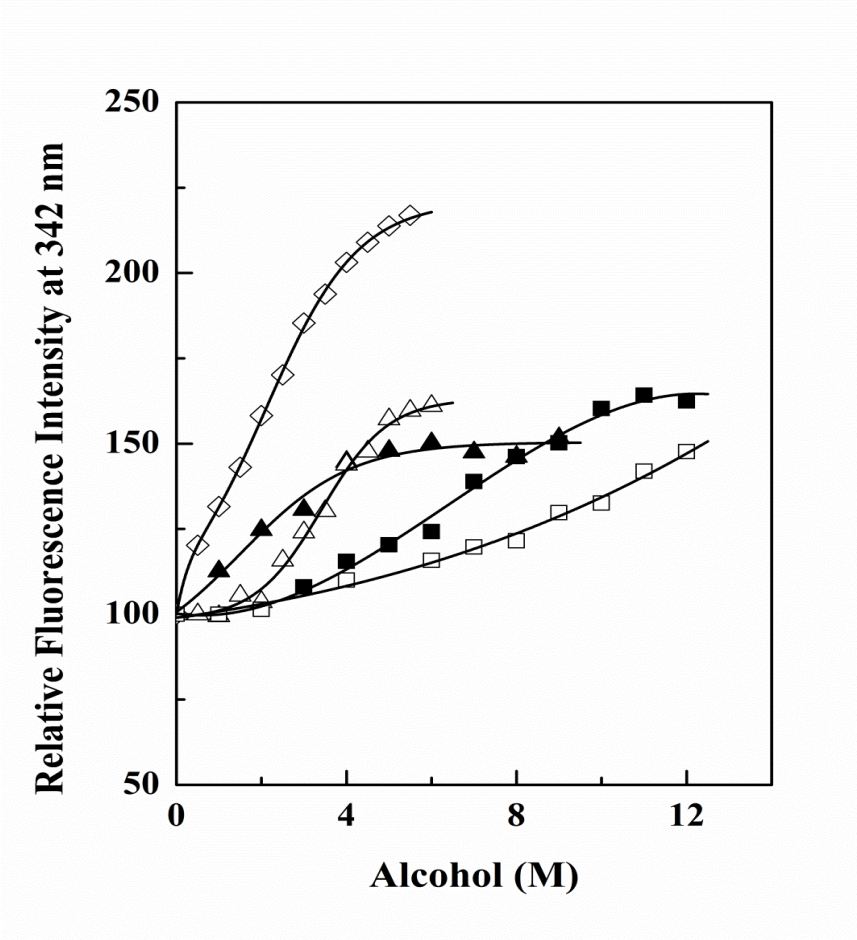

Figure 4.24. Conformational transitions of the acid-denatured glucoamylase at pH 1.0 (25ºC) induced by alkanols as monitored by Trp fluorescence measurements at 342 nm (excitation wavelength = 295 nm), using a protein concentration of 0.12 μM. Various symbols shown in the figure refer to: tert-butanol (◊), 1-propanol (▲), 2-propanol (Δ), ethanol (■) and methanol (□).

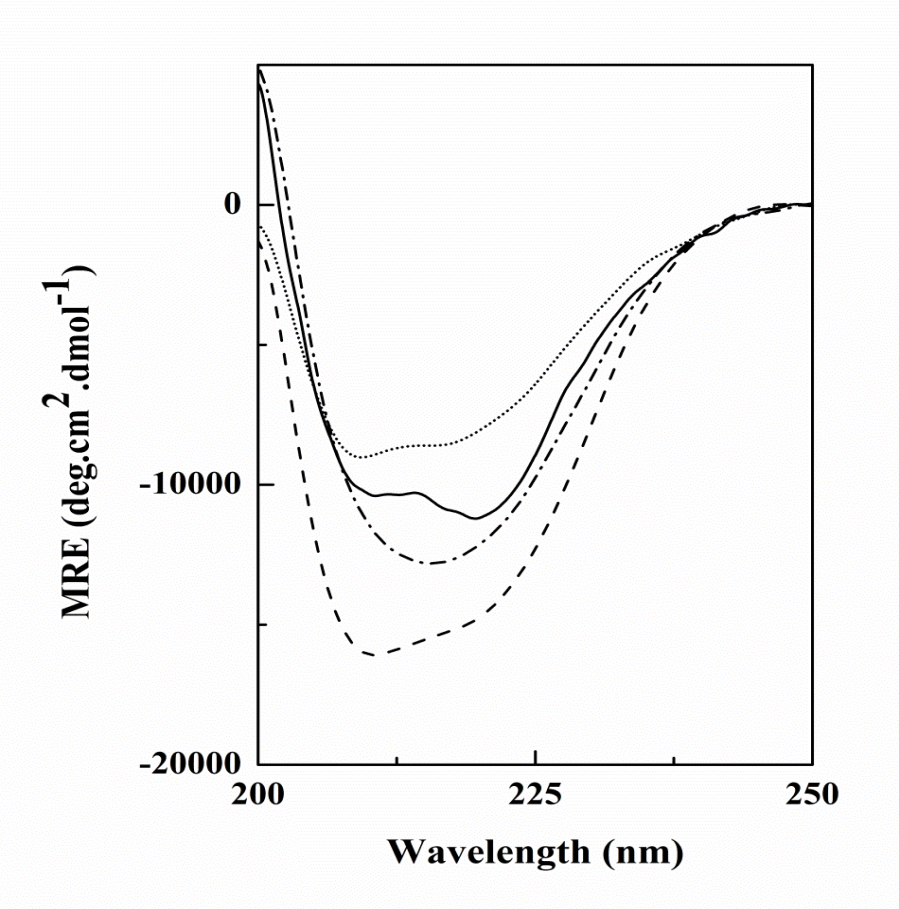

Figure 4.25. Far-UV CD spectra of the native glucoamylase in 10 mM sodium phosphate buffer, pH 7.0 (——) and the acid-denatured glucoamylase both in the absence (·····) and presence of 7.0 M TFE (– – –) or 5.5 M tert-butanol (– · –). The spectra were recorded at 25ºC, using a protein concentration of 1.4 μM.

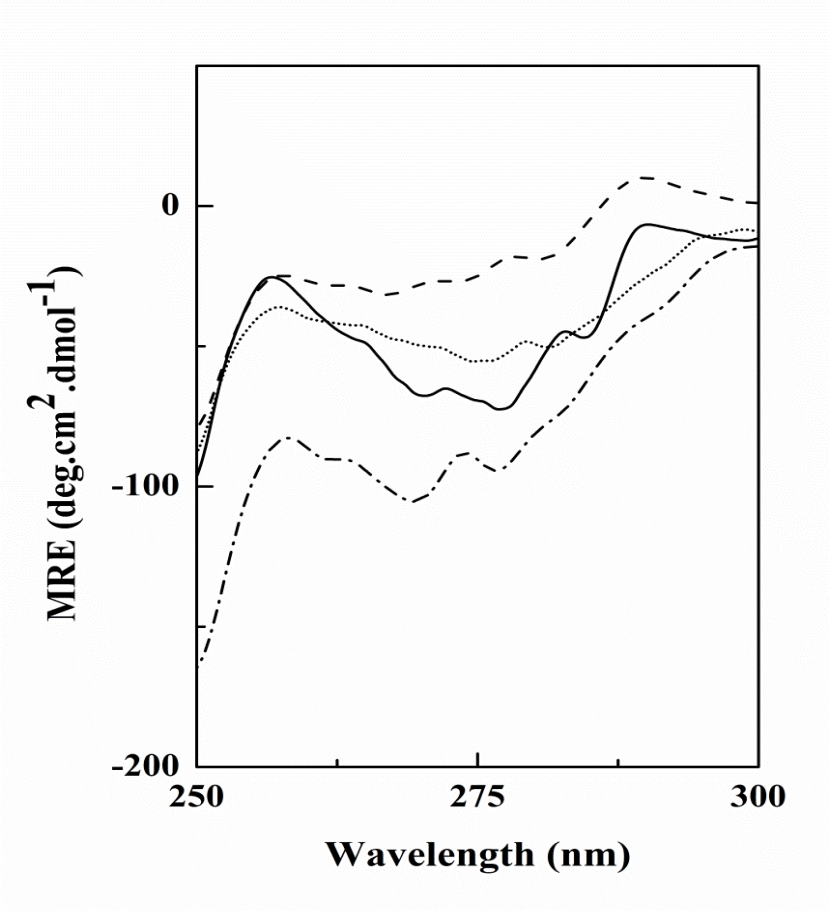

Figure 4.26. Near-UV CD spectra of the native glucoamylase in 10 mM sodium phosphate buffer, pH 7.0 (——) and the acid-denatured glucoamylase both in the absence (·····) and presence of 7.0 M TFE (– – –) or 5.5 M tert-butanol (– · –). The spectra were recorded at 25ºC, using a protein concentration of 12.0 μM.

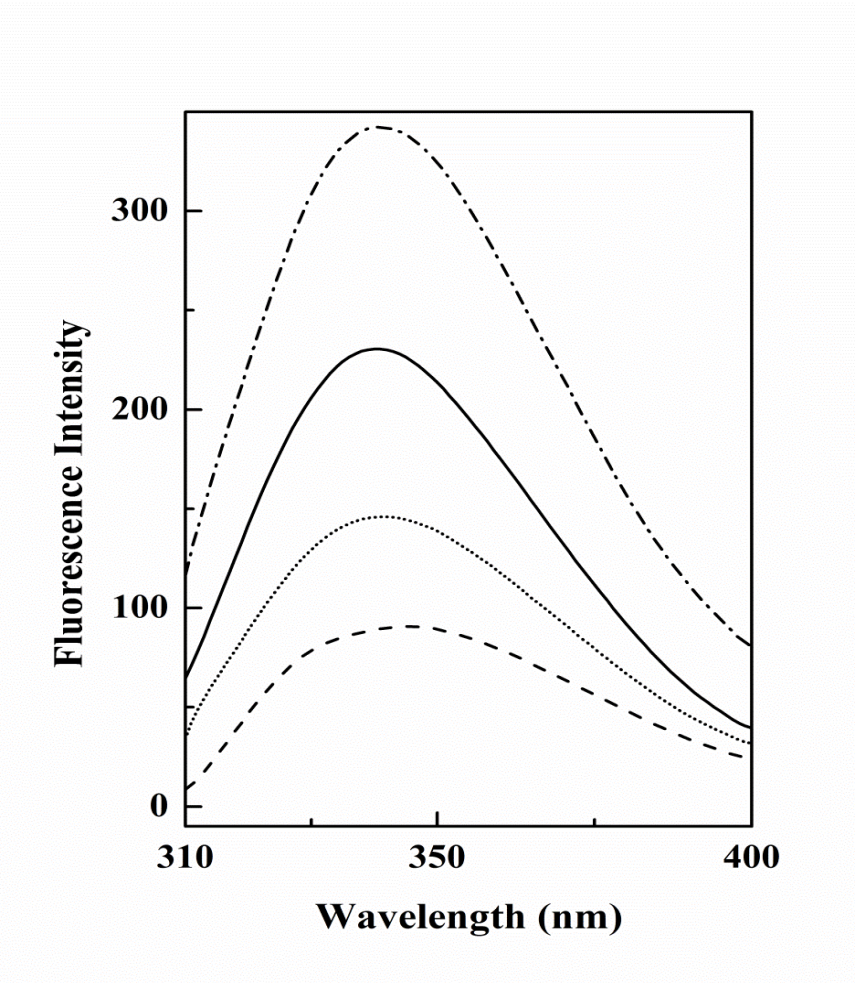

Figure 4.27. Tryptophan fluorescence spectra of the native (——) and the acid-denatured glucoamylases both in the absence (·····) and presence of 7.0 M TFE (– – –) or 5.5 M tert-butanol (– · –). The spectra were recorded at 25ºC, using a protein concentration of 0.12 μM.

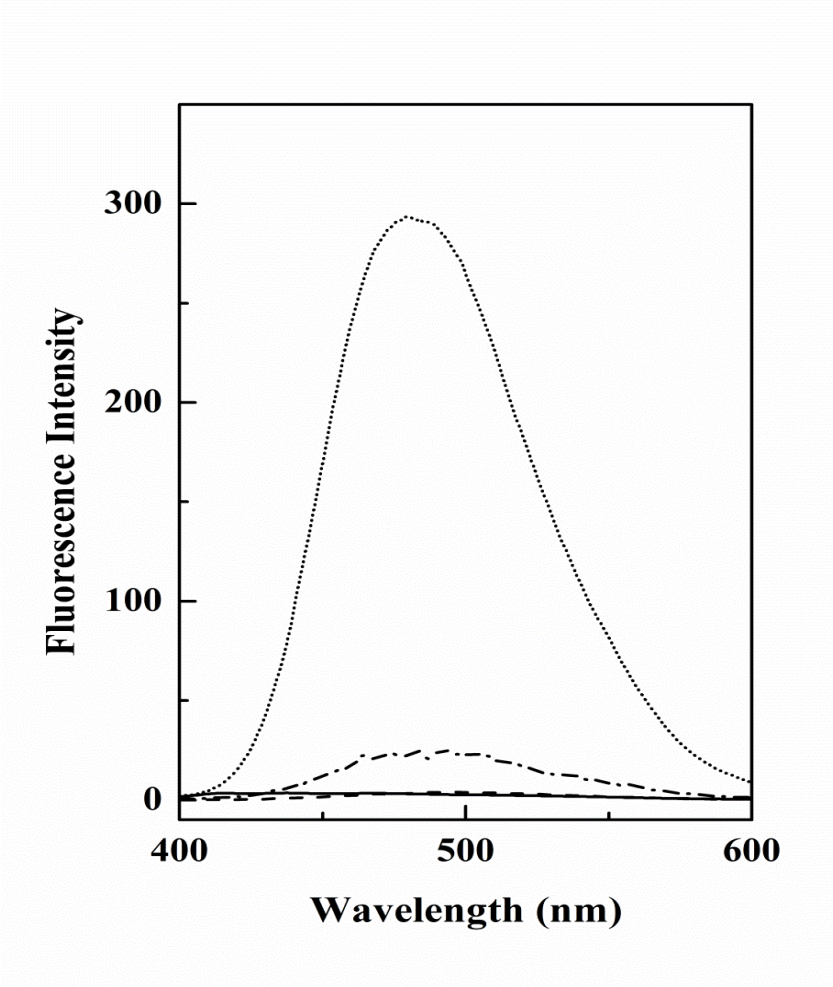

Figure 4.28. ANS fluorescence spectra of the native (——) and the acid-denatured glucoamylases both in the absence (·····) and presence of 5.0 M TFE (– – –) or 5.0 M tert-butanol (– · –).The spectra were recorded at 25ºC, using a protein concentration of 0.26 μM.

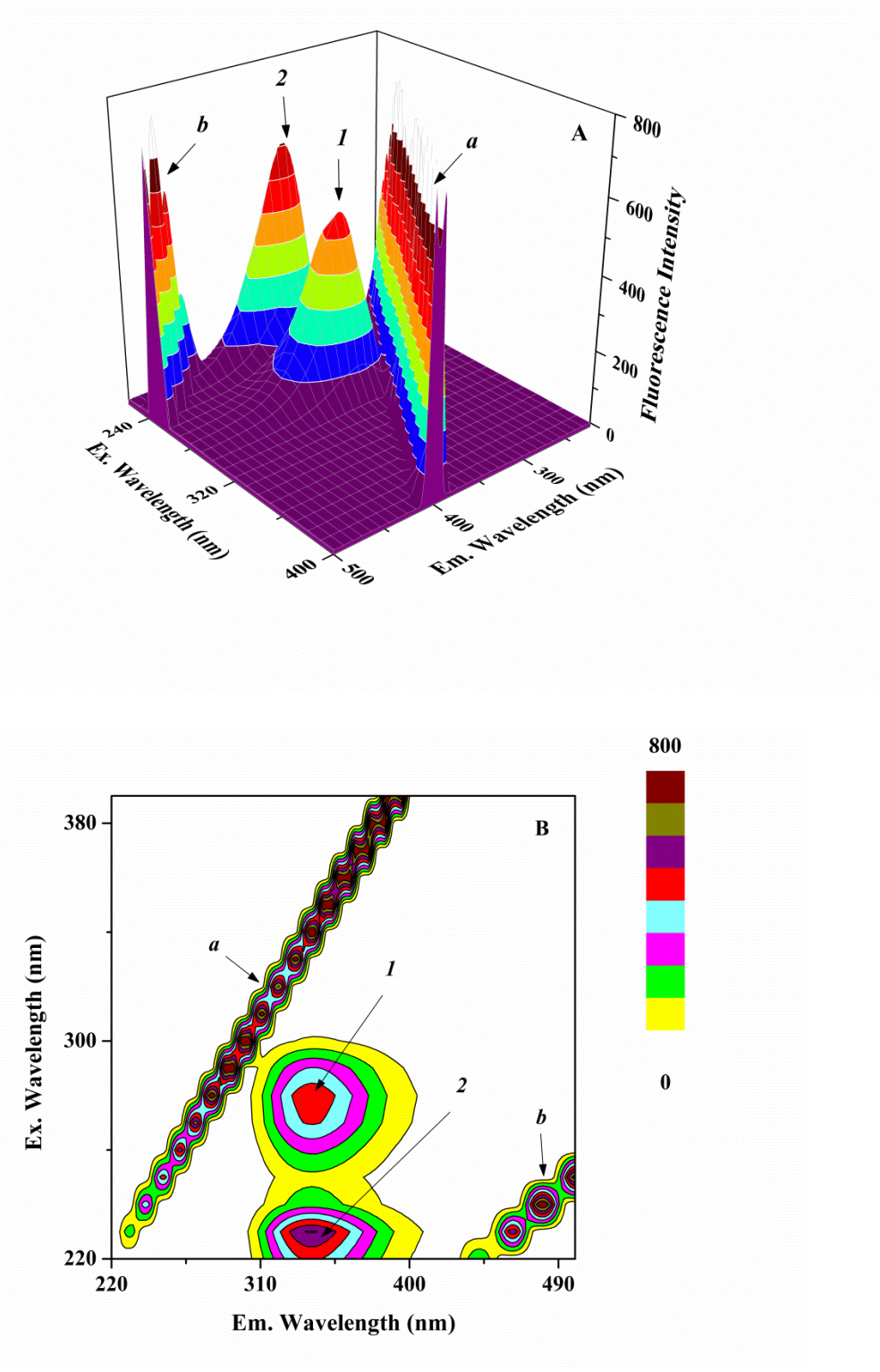

Figure 4.29. Three-dimensional fluorescence spectra (A) and corresponding contour map (B) of the native glucoamylase. The protein concentration used was 0.13 μM.

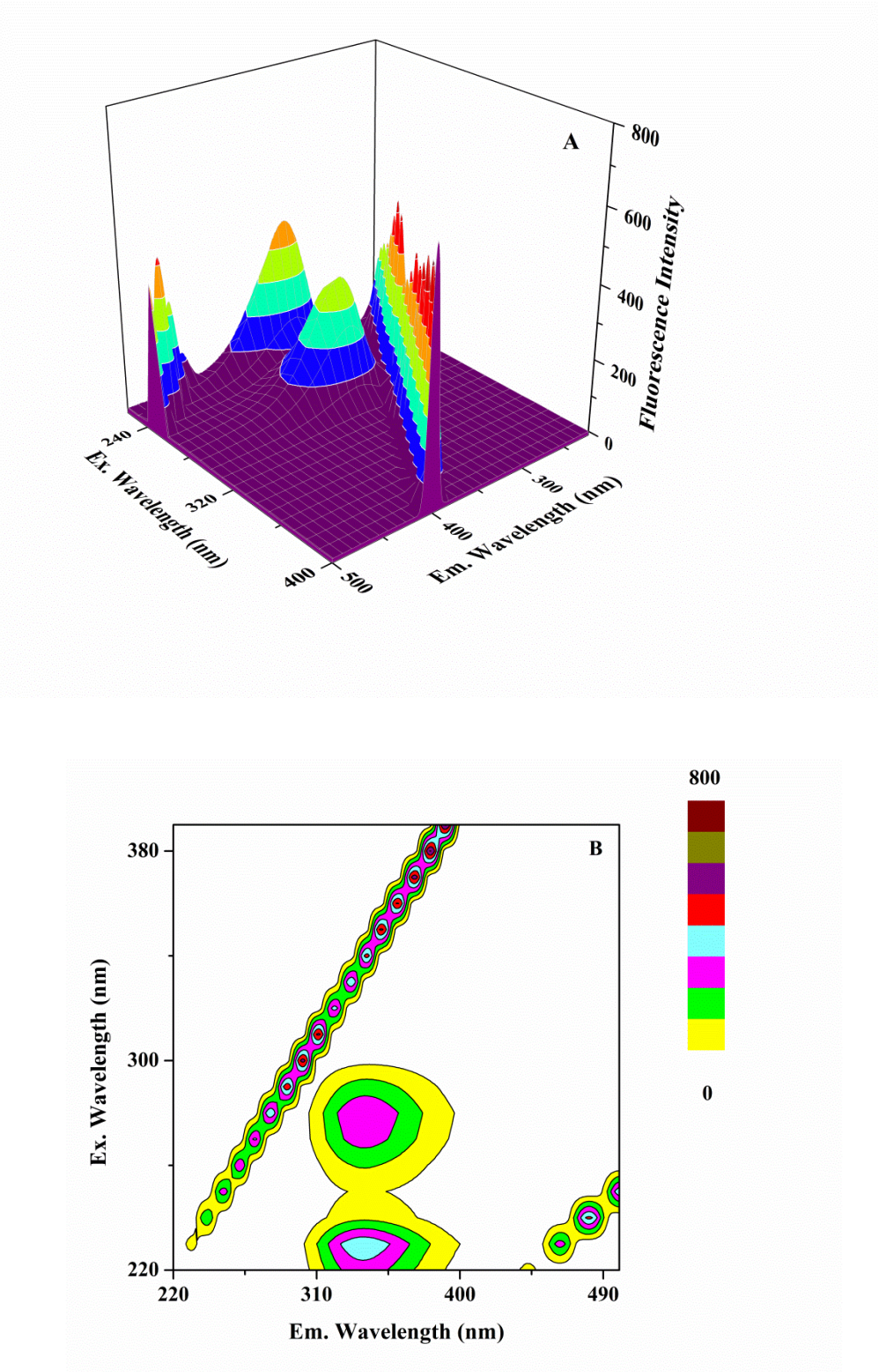

Figure 4.30. Three-dimensional fluorescence spectra (A) and corresponding contour map (B) of the acid-denatured glucoamylase. The protein concentration used was 0.13 μM.

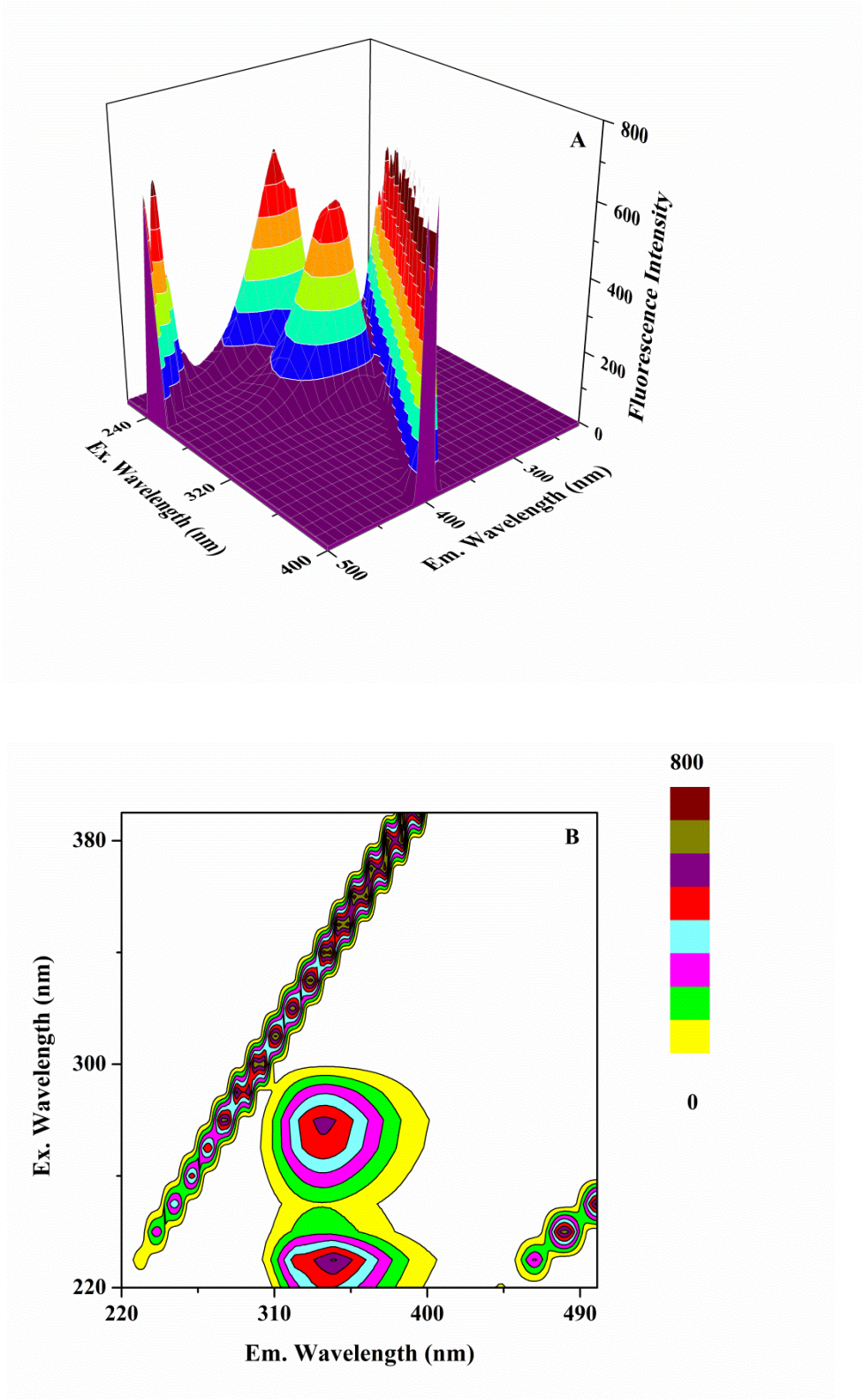

Figure 4.31. Three-dimensional fluorescence spectra (A) and corresponding contour map (B) of the acid-denatured glucoamylase in the presence of 5.5 M tert-butanol. The protein concentration used was 0.13 μM.

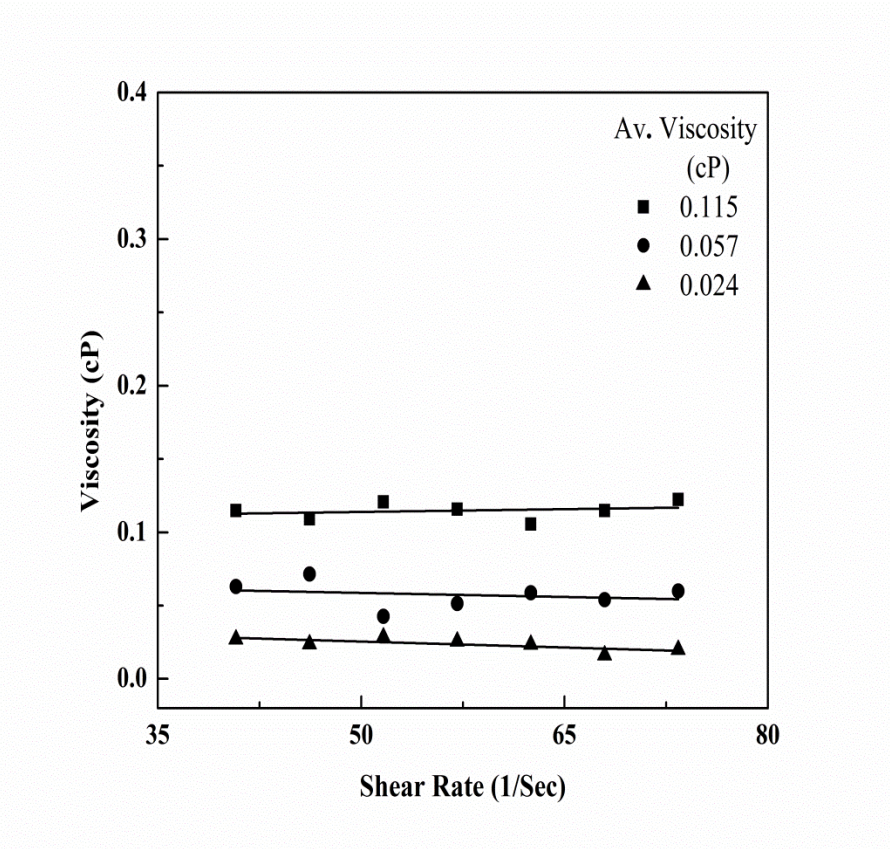

Figure 4.32. Viscosity versus shear rate plots of the native glucoamylase (▲) and the acid-denatured glucoamylase both in the absence (■) and presence (●) of 8.0 M TFE. The experiments were performed at 25ºC using 15 ml of the protein solution (13.75 μM).

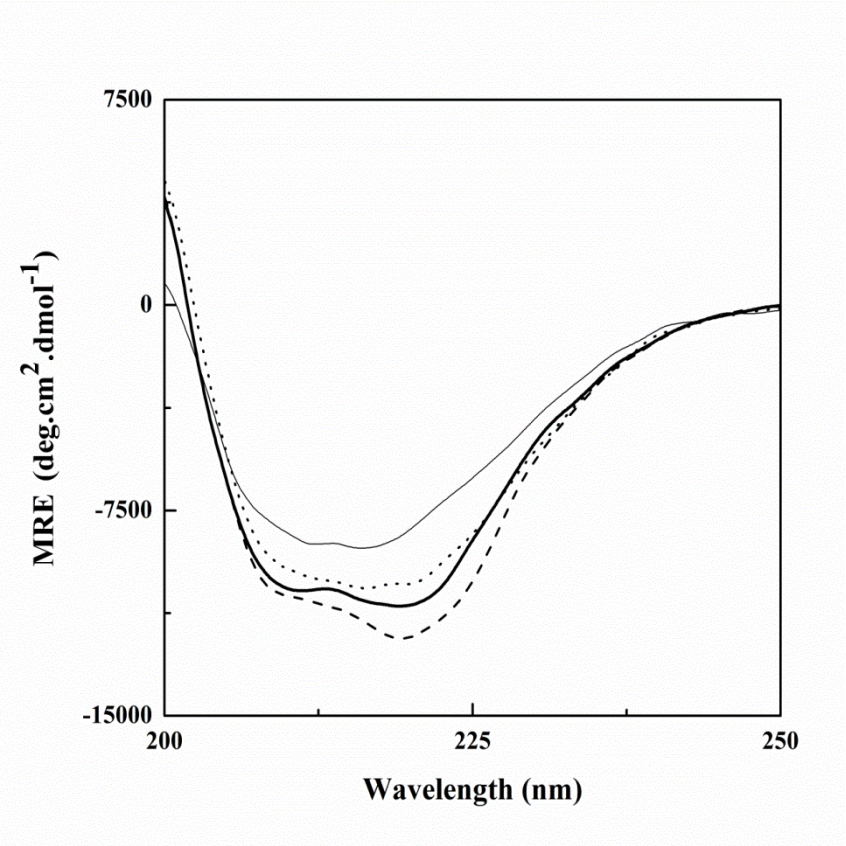

Figure 4.33. Effect of glucose on the far-UV CD spectra of the native and the acid-denatured glucoamylases. Different line symbols represent: native glucoamylase (——), acid-denatured glucoamylase (——), native glucoamylase + 2.6 M glucose (– – –) and acid-denatured glucoamylase + 2.6 M glucose (.....). The spectra were recorded at 25˚C using a protein concentration of 1.4 μM.

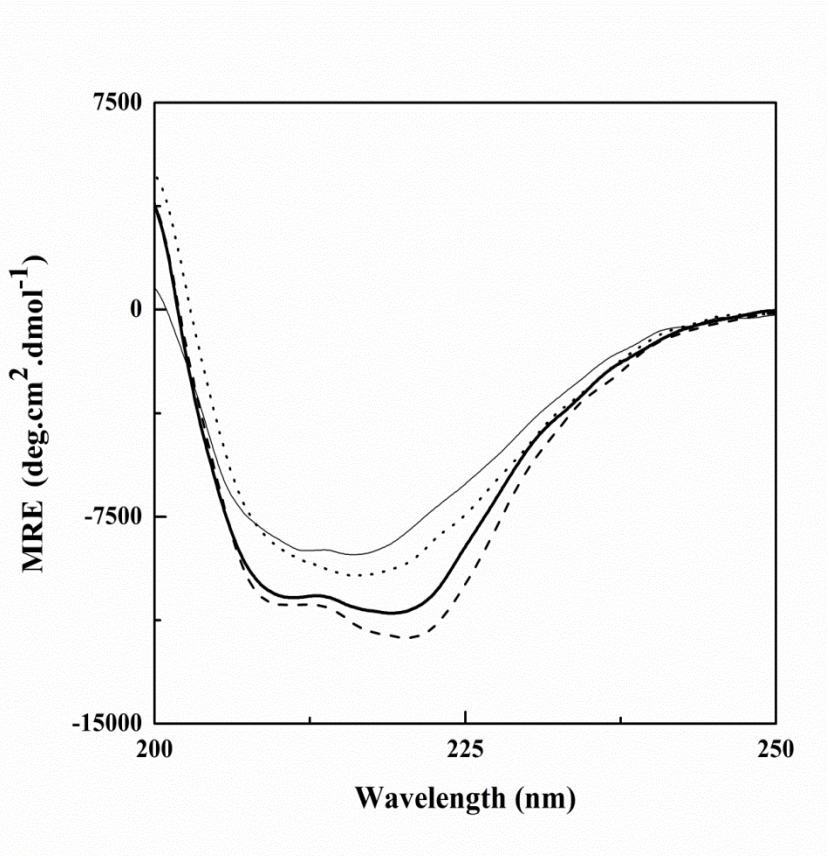

Figure 4.34. Effect of trehalose on the far-UV CD spectra of the native and the acid-denatured glucoamylases. Different line symbols represent: native glucoamylase (——), acid-denatured glucoamylase (——), native glucoamylase + 1.3 M trehalose (– – –) and acid-denatured glucoamylase + 1.3 M trehalose (.....). The spectra were recorded at 25˚C using a protein concentration of 1.4 μM.

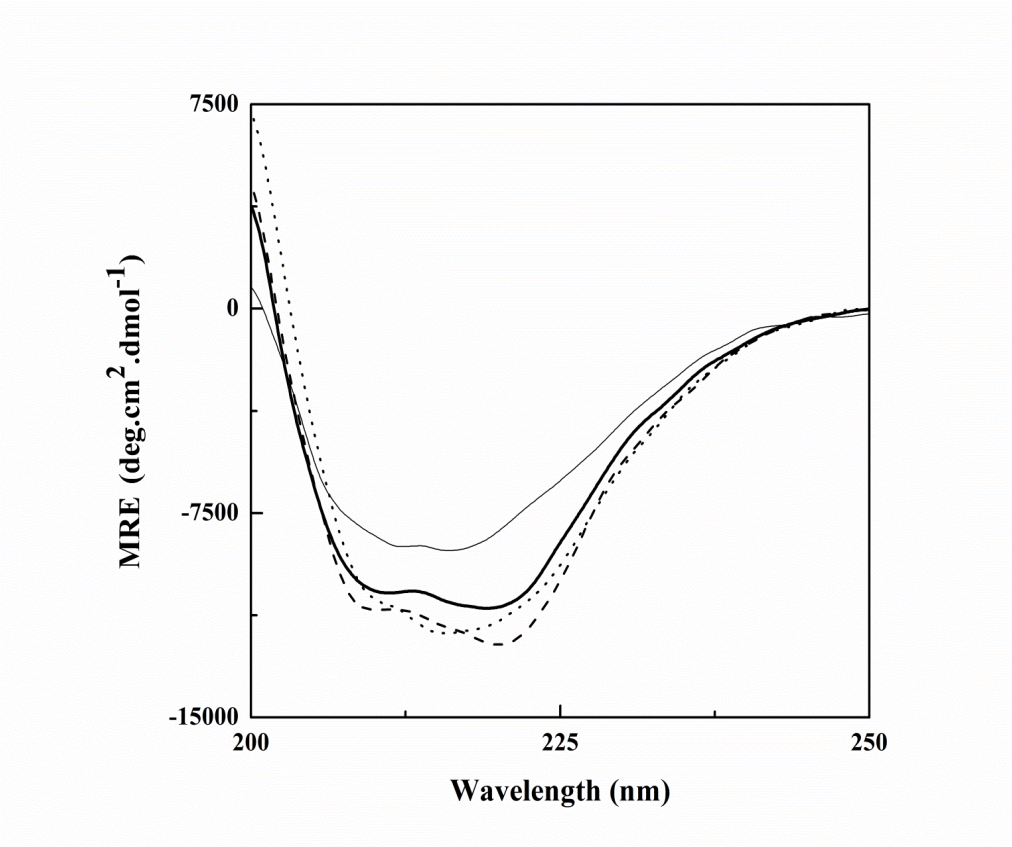

Figure 4.35. Effect of glycerol on the far-UV CD spectra of the native and the acid-denatured glucoamylases. Different line symbols represent: native glucoamylase (——), acid-denatured glucoamylase (——), native glucoamylase + 8.0 M glycerol (– – –) and acid-denatured glucoamylase + 8.0 M glycerol (.....). The spectra were recorded at 25˚C using a protein concentration of 1.4 μM.

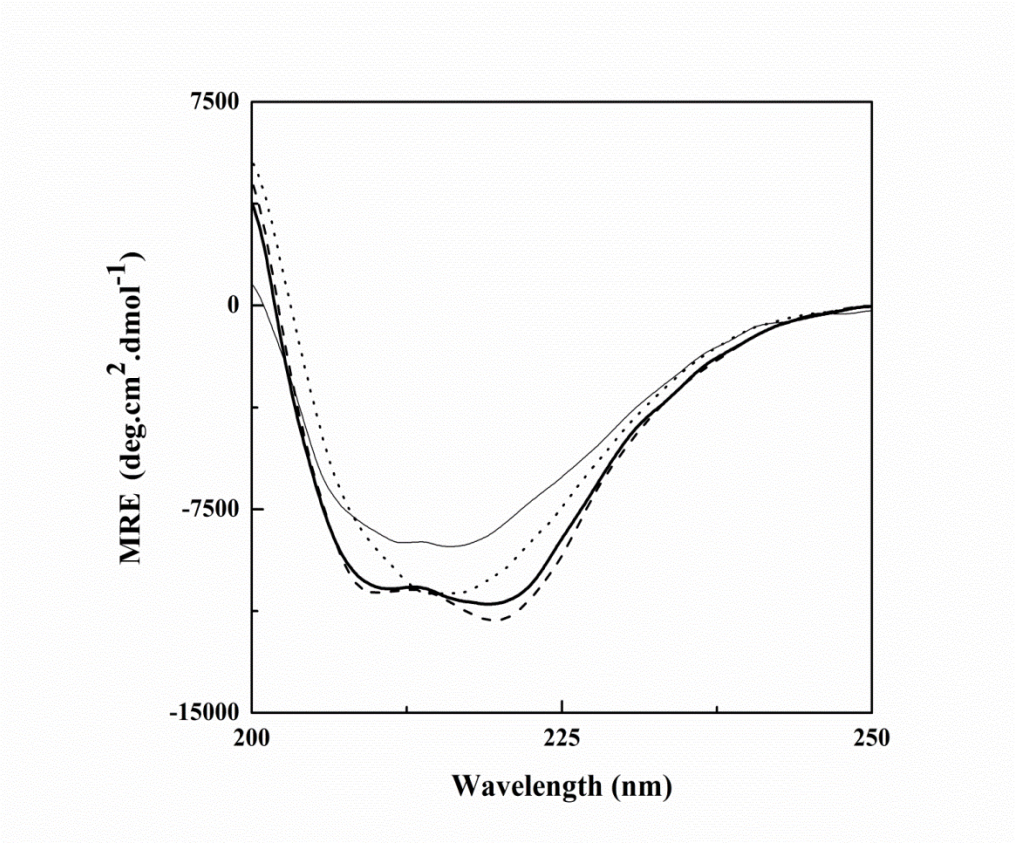

Figure 4.36. Effect of ethylene glycol on the far-UV CD spectra of the native and the acid-denatured glucoamylases. Different line symbols represent: native glucoamylase (——), acid-denatured glucoamylase (——), native glucoamylase + 8.0 M ethylene glycol (– – –) and acid-denatured glucoamylase + 8.0 M ethylene glycol (.....). The spectra were recorded at 25˚C using a protein concentration of 1.4 μM.

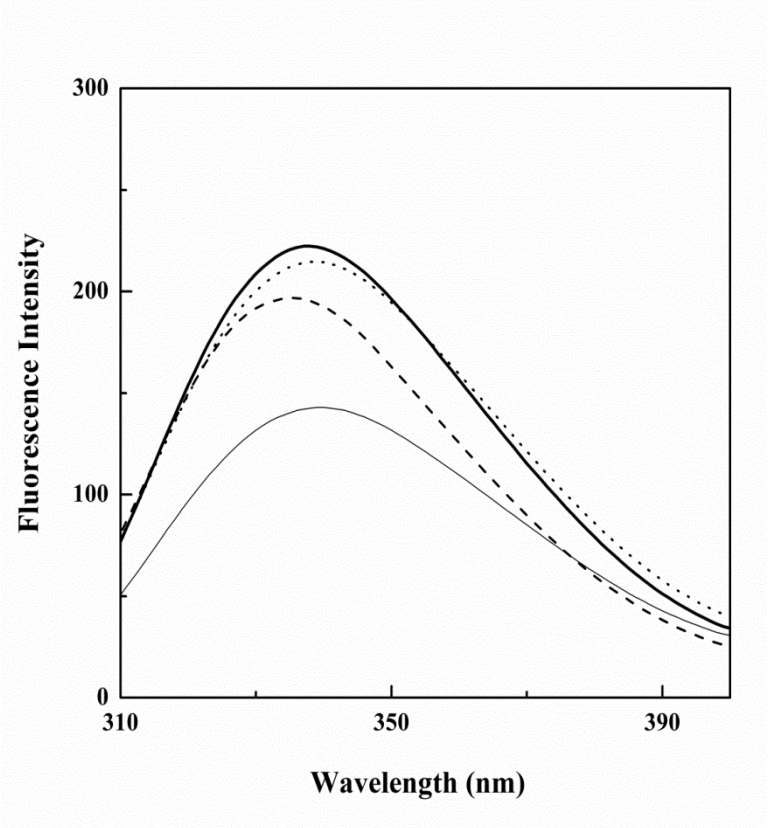

Figure 4.37. Effect of glucose on the tryptophan fluorescence spectra of the native and the acid-denatured glucoamylases. Different line symbols represent: native glucoamylase (——), acid-denatured glucoamylase (——), native glucoamylase + 2.6 M glucose (– – –) and acid-denatured glucoamylase + 2.6 M glucose (.....). The spectra were recorded at 25˚C using a protein concentration of 0.12 μM.

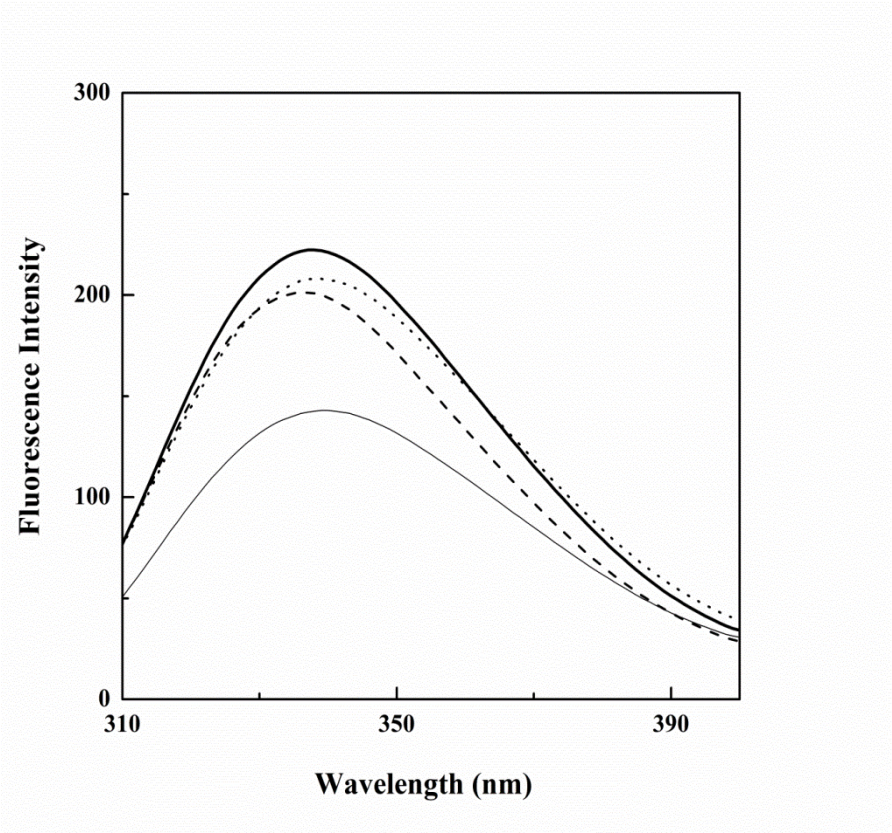

Figure 4.38. Effect of trehalose on the tryptophan fluorescence spectra of the native and the acid-denatured glucoamylases. Different line symbols represent: native glucoamylase (——), acid-denatured glucoamylase (——), native glucoamylase + 1.3 M trehalose (– – –) and acid-denatured glucoamylase + 1.3 M trehalose (.....). The spectra were recorded at 25˚C using a protein concentration of 0.12 μM.

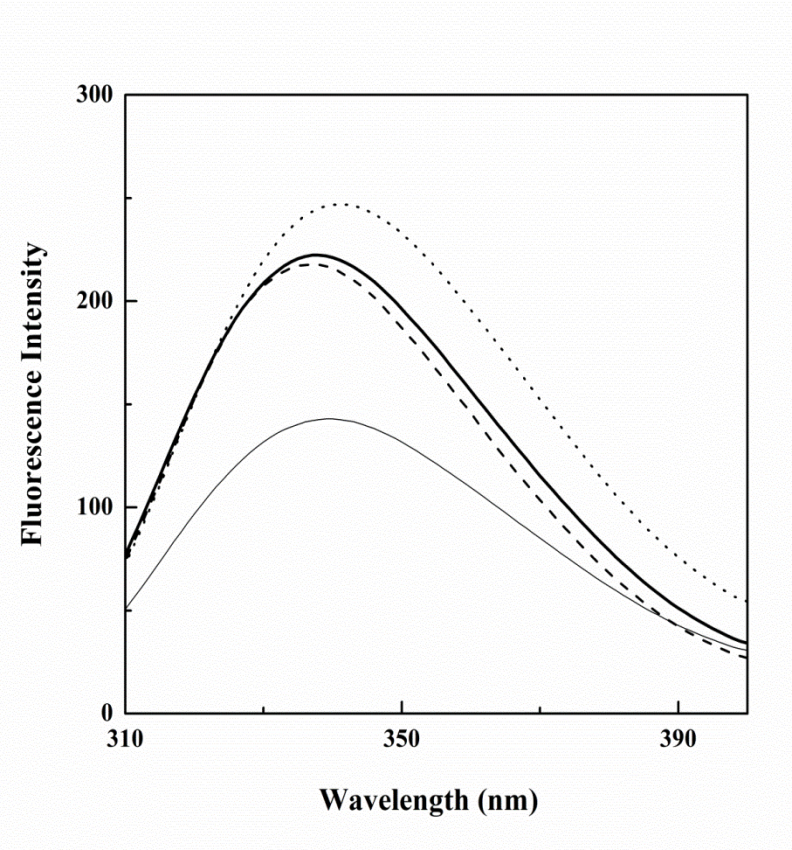

Figure 4.39. Effect of glycerol on the tryptophan fluorescence spectra of the native and the acid-denatured glucoamylases. Different line symbols represent: native glucoamylase (——), acid-denatured glucoamylase (—), native glucoamylase + 8.0 M glycerol (– – –) and acid-denatured glucoamylase + 8.0 M glycerol (.....). The spectra were recorded at 25˚C using a protein concentration of 0.12 μM.

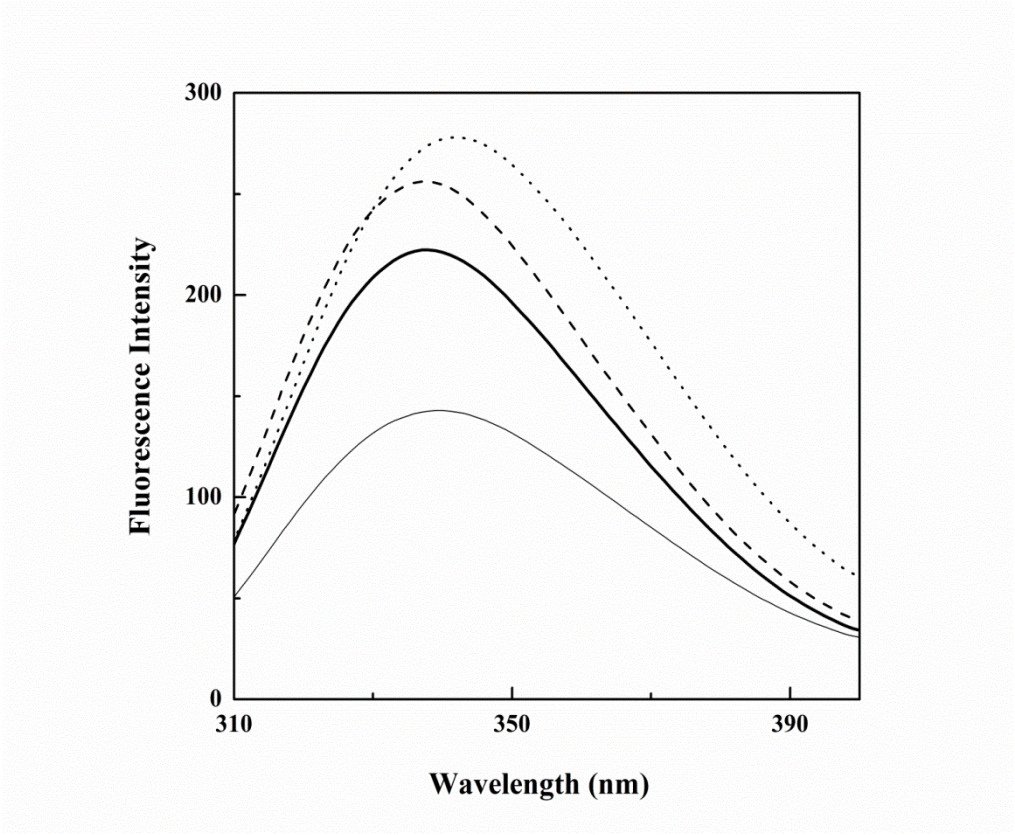

Figure 4.40. Effect of ethylene glycol on the tryptophan fluorescence spectra of the native and the acid-denatured glucoamylases. Different line symbols represent: native glucoamylase (——), acid-denatured glucoamylase (——), native glucoamylase + 8.0 M ethylene glycol (– – –) and acid-denatured glucoamylase + 8.0 M ethylene glycol (.....). The spectra were recorded at 25˚C using a protein concentration of 0.12 μM.

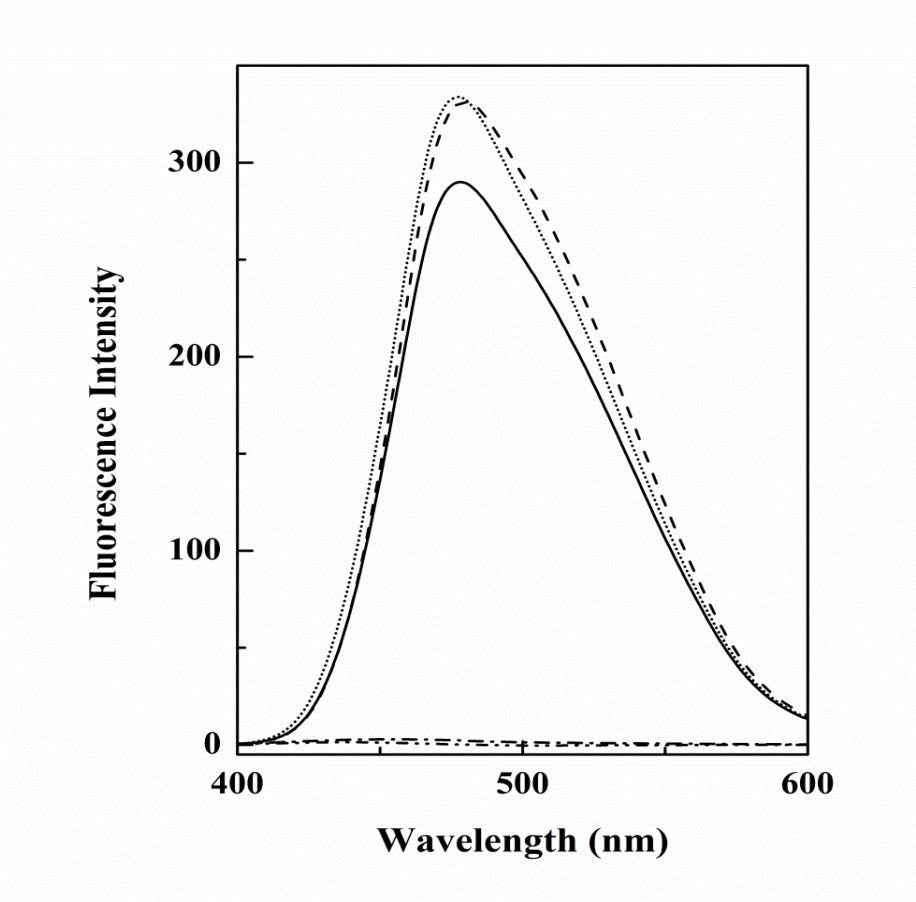

Figure 4.41. ANS fluorescence spectra of the acid-denatured glucoamylase in the absence (——) and presence of 2.6 M glucose (– – –), 1.3 M trehalose (.....), 8.0 M glycerol (– · – ·) and 8.0 M ethylene glycol (— · · —). The spectra were recorded at 25˚C, using a protein concentration of 0.26 μM and [ANS]/[protein] molar ratio as 70:1.

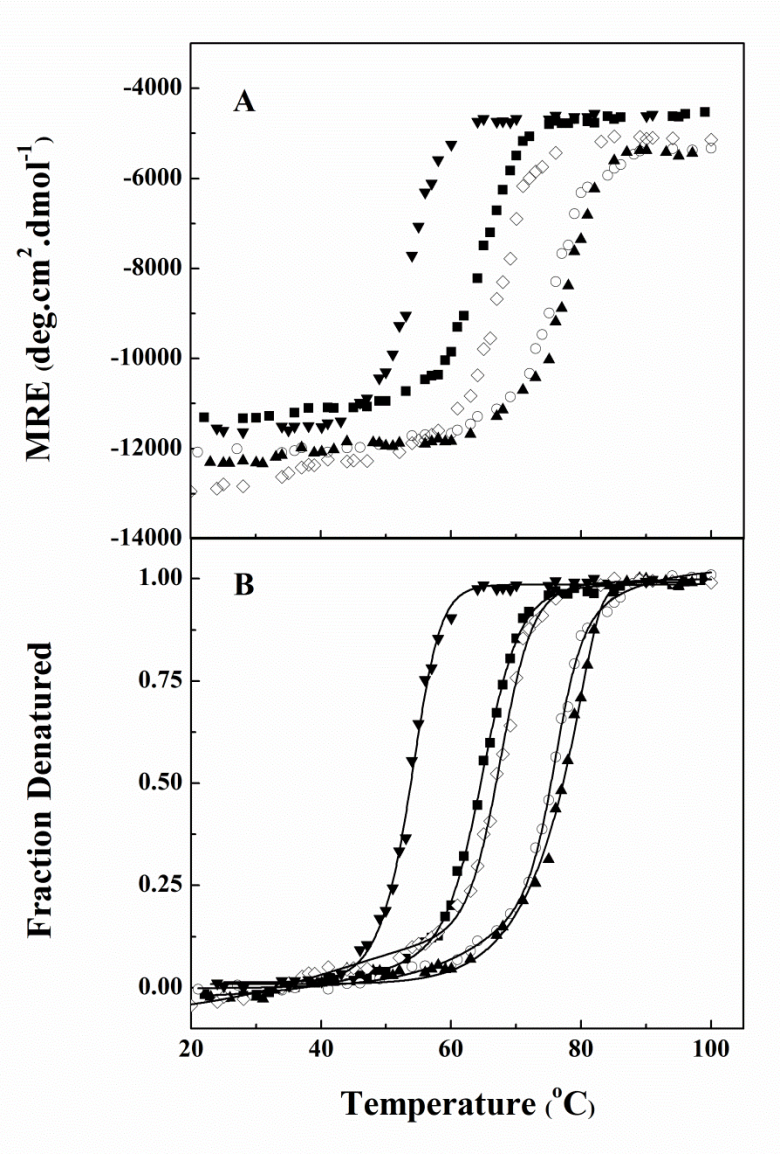

Figure 4.42. Thermal transition curves (A) and corresponding normalized curves (B) of the native glucoamylase in the absence (■) and presence of 2.6 M glucose (▲), 1.3 M trehalose (○), 8.0 M glycerol (◊) and 8.0 M ethylene glycol (▼) as monitored by MRE_{222nm} measurements, using a protein concentration of 1.4 μM.

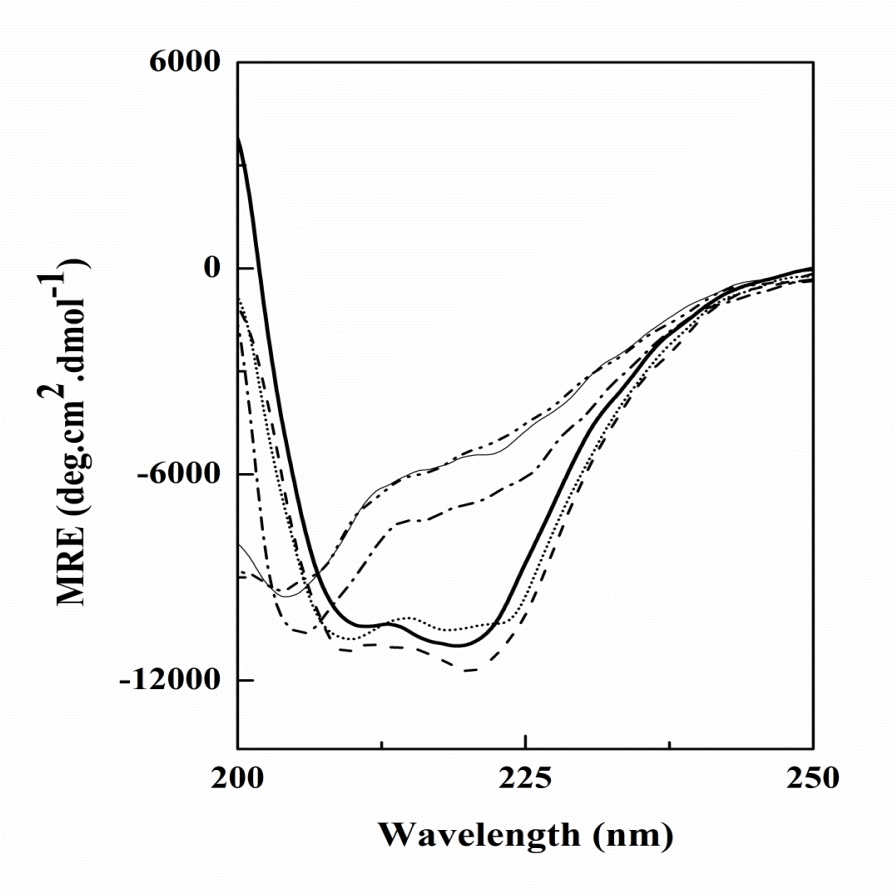

Figure 4.43. Far-UV CD spectra of the native (——) and the thermal-denatured glucoamylases in the absence (——) and presence of 2.6 M glucose (– – –), 1.3 M trehalose (.....), 8.0 M glycerol (– . – .) and 8.0 M ethylene glycol (— . . —). The spectra of thermal-denatured glucoamylase were recorded after equilibrating the sample at 71˚C for 6 min, using a protein concentration of 1.4 μM.

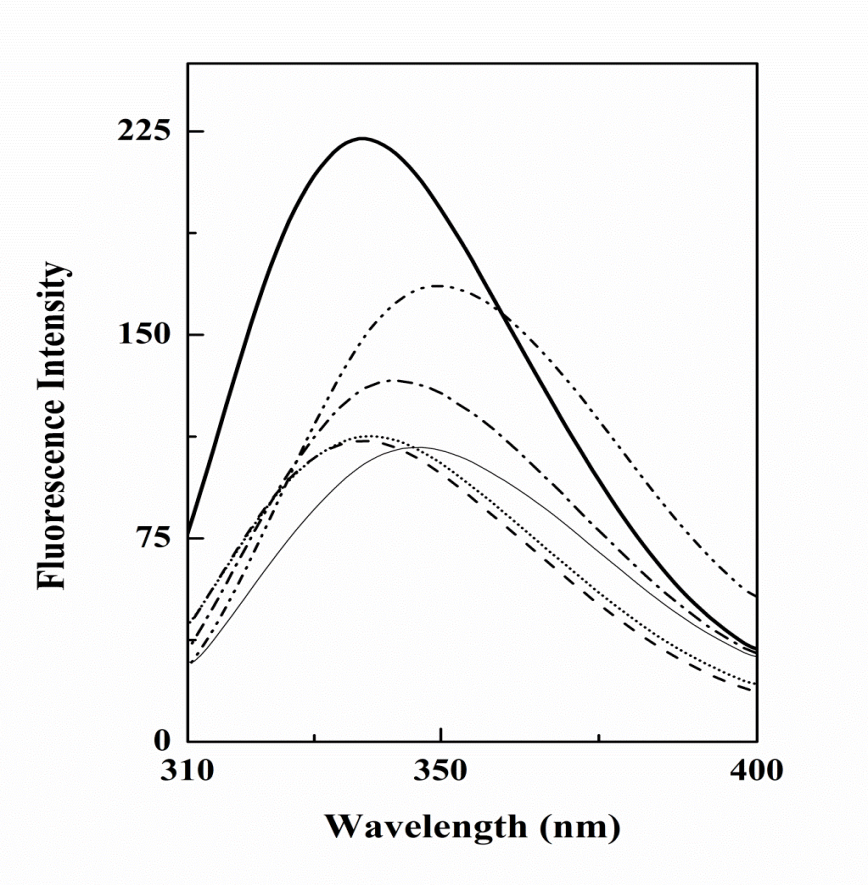

Figure 4.44. Tryptophan fluorescence spectra of the native (——) and the thermal-denatured glucoamylases in the absence (——) and presence of 2.6 M glucose (– – –), 1.3 M trehalose (.....), 8.0 M glycerol (– · – ·) and 8.0 M ethylene glycol (— · · —). The spectra of thermal-denatured glucoamylase were recorded after equilibrating the sample at 71˚C for 6 min, using a protein concentration of 0.12 μM.